NASA/TM—2001-210897

Computational Thermodynamic Study to Predict Complex Phase Equilibria in the Nickel-Base Superalloy René N6

Evan H. Copland, Nathan S. Jacobson, and Frank J. Ritzert
Glenn Research Center, Cleveland, Ohio

September 2001

The NASA STI Program Office . . . in Profile

Since its founding, NASA has been dedicated to the advancement of aeronautics and space science. The NASA Scientific and Technical Information (STI) Program Office plays a key part in helping NASA maintain this important role.

The NASA STI Program Office is operated by Langley Research Center, the Lead Center for NASA's scientific and technical information. The NASA STI Program Office provides access to the NASA STI Database, the largest collection of aeronautical and space science STI in the world. The Program Office is also NASA's institutional mechanism for disseminating the results of its research and development activities. These results are published by NASA in the NASA STI Report Series, which includes the following report types:

- TECHNICAL PUBLICATION. Reports of completed research or a major significant phase of research that present the results of NASA programs and include extensive data or theoretical analysis. Includes compilations of significant scientific and technical data and information deemed to be of continuing reference value. NASA's counterpart of peer-reviewed formal professional papers but has less stringent limitations on manuscript length and extent of graphic presentations.

- TECHNICAL MEMORANDUM. Scientific and technical findings that are preliminary or of specialized interest, e.g., quick release reports, working papers, and bibliographies that contain minimal annotation. Does not contain extensive analysis.

- CONTRACTOR REPORT. Scientific and technical findings by NASA-sponsored contractors and grantees.

- CONFERENCE PUBLICATION. Collected papers from scientific and technical conferences, symposia, seminars, or other meetings sponsored or cosponsored by NASA.

- SPECIAL PUBLICATION. Scientific, technical, or historical information from NASA programs, projects, and missions, often concerned with subjects having substantial public interest.

- TECHNICAL TRANSLATION. English-language translations of foreign scientific and technical material pertinent to NASA's mission.

Specialized services that complement the STI Program Office's diverse offerings include creating custom thesauri, building customized data bases, organizing and publishing research results . . . even providing videos.

For more information about the NASA STI Program Office, see the following:

- Access the NASA STI Program Home Page at ***http://www.sti.nasa.gov***

- E-mail your question via the Internet to help@sti.nasa.gov

- Fax your question to the NASA Access Help Desk at 301–621–0134

- Telephone the NASA Access Help Desk at 301–621–0390

- Write to:
  NASA Access Help Desk
  NASA Center for AeroSpace Information
  7121 Standard Drive
  Hanover, MD 21076

NASA/TM—2001-210897

Computational Thermodynamic Study to Predict Complex Phase Equilibria in the Nickel-Base Superalloy René N6

Evan H. Copland, Nathan S. Jacobson, and Frank J. Ritzert
Glenn Research Center, Cleveland, Ohio

National Aeronautics and
Space Administration

Glenn Research Center

September 2001

Acknowledgments

We thank N. Saunders of Thermotech, Surrey, UK and T. Gabb of NASA Glenn for their helpful comments. We also thank R. Garlick for X-ray diffraction and J. Smith for microprobe.

Available from

NASA Center for Aerospace Information
7121 Standard Drive
Hanover, MD 21076

National Technical Information Service
5285 Port Royal Road
Springfield, VA 22100

Available electronically at http://gltrs.grc.nasa.gov/GLTRS

COMPUTATIONAL THERMODYNAMIC STUDY TO PREDICT COMPLEX PHASE EQUILIBRIA IN THE NICKEL-BASE SUPERALLOY RENÉ N6

Evan H. Copland,* Nathan S. Jacobson, and Frank Ritzert
National Aeronautics and Space Administration
Glenn Research Center
Cleveland, Ohio 44135

SUMMARY

A previous study by Ritzert et al. (refs. 1 and 2) on the formation and prediction of topologically closed packed (TCP) phases in the nickel-base superalloy René N6 is re-examined with computational thermodynamics. The experimental data on phase distribution in forty-four alloys with a composition within the patent limits of the nickel-base superalloy René N6 provide a good basis for comparison to and validation of a commercial nickel superalloy database[1] (ref. 3) used with ThermoCalc[2] (ref. 4). Volume fraction of the phases and partitioning of the elements are determined for the forty-four alloys in this dataset. The baseline heat treatment of 400 h at 1366 K was used. This composition set is particularly interesting since small composition differences lead to dramatic changes in volume fraction of each phase. In general the calculated values follow the experimental trends. However, the calculations indicated no TCP phase formation when the experimental measurements gave a volume percent of TCP phase less than 2 percent. When TCP phases were predicted, the calculations under-predict the volume percent of TCP phases by a factor of 2 to 8. The calculated compositions of the γ and γ' phases show fair agreement with the measurements. However, the calculated compositions of the P Phase do not agree with those measured. This may be due to inaccuracies in the model parameters for P phase and/or issues with the microprobe analyses of these phases. In addition, phase fraction diagrams and σ and P phase solvus temperatures are calculated for each of the alloys. These calculations indicate that P phase is the primary TCP phase formed for the alloys considered here at 1366 K. Finally, a series of isopleths are calculated for each of the seven alloying elements. These show the effect of each alloying element on creating TCP phases.

INTRODUCTION

Modern third and fourth generation superalloys involve the addition of various refractory elements for improved creep rupture strength. The addition of rhenium (Re) seems particularly promising (ref. 5). A problem with the introduction of refractory metals is that they increase the stability of topologically closed packed (TCP) phases. These phases are detrimental due to both their brittleness and the fact that they deplete the matrix of solid solution strengthening elements (ref. 6 and 7). Table I lists the four commonly observed TCP phases and their lattice parameters (ref. 6).

Ritzert et al. (refs. 1 and 2) have recently reported a study of TCP phase precipitation in compositions of the nickel-base superalloy René N6. Forty-four compositions in a range within the patent limitations of the superalloy René N6 were prepared. This composition set contained thirty-four variations with ten repeats, according to a design of experiments (DOE) approach. These compositions are given in table II. The compositions included only the elements Ni-Co-Al-Cr-Mo-W-Re-Ta. Although commercial René N6 also contains C, B, Hf, Ti, and V; these elements were omitted from the composition set to reduce the number of alloys in this study and accentuate some phase formation effects. In particular, the omission of C, which tends to tie up refractory elements as carbides, allowed formation of TCP phases more readily for the purpose of their study.

---

*National Research Council—NASA Research Associate at Glenn Research Center.
[1]NI-DATA, Thermotech Ltd., Surrey, UK.
[2]ThermoCalc AB, Stockholm, Sweden.

TABLE I.—CRYSTALLOGRAPHIC INFORMATION ON THE TCP PHASES FROM RAE et al. (ref. 6)

TCP phase	System	Atoms per unit cell	Lattice parameter	α
σ	Tetragonal	30	a = b = 0.878 nm c = 0.454 nm	90°
P	Orthorhombic	56	a = 1.698 nm b = 0.475 nm c = 0.907 nm	90°
μ	Rhombohedral	13 (hex. 39)	a = b = c = 0.904 nm a = b = 0.4755 nm c = 2.583 nm	30.5° 120°
R	Rhombohedral	53 (hex. 159)	a = b = 0.4755 nm c = 2.583 nm	120°

Ritzert et al. (refs. 1 and 2) cast and homogenized the alloys at 1315 °C (1588 K) for 80 hrs. Then they heat treated the alloys at 1093 °C (1366 K) for 400 hrs. They examined the alloys with X-ray diffraction (XRD), scanning electron microscopy (SEM), and electron microprobe (EPMA). Ritzert et al. (refs. 1 and 2) determined both the volume fraction and distribution of the TCP phases in the microstructure. This allowed classification of the alloys into three categories, depending on the volume fraction and morphology with relation to the grain boundaries of the TCP phases. They also determined lattice parameters of the γ' phase and the P phase, when possible. From the data on volume fraction of TCP phases, Ritzert et al. (refs. 1and 2) developed a predictive equation for the formation of TCP phases.

Today computational thermodynamics has advanced to the point of predicting the equilibrium phases observed in many commercial alloys (refs. 5 to 7). The Ni-database developed by Saunders et al. (refs. 3 and7) contains up to 14 elements and 17 phases, as listed in table III. This database together with the ThermoCalc Code (ref. 4) are used in this study to model the phase formation in the alloys examined by Ritzert et al. (refs. 1 and 2). The direct comparison of the thermodynamic calculations with experiments also permits validation of the database and this approach in general.

The ThermoCalc Code is a computational thermodynamics package based on free energy minimization, capable of a variety of thermodynamic calculations. ThermoCalc consists of a series of modules. The database module inputs the data for each phase in the form of a free energy curve as a function of composition and temperature, $G_m^P(x,T)$. Note that pressure does not enter into these expressions. For current alloy modeling studies, the pressure is fixed at one bar (101325 Pa). The free energy is in the form (ref. 8):

$$G_m^p(x,T) = G_m^{ref} - TS_m^{ideal} + {}^E G_m \tag{1}$$

Here G_m^{ref} is the weighted sum of the free energies for each component:

$$G_m^{ref} = \sum_{i=1}^{n} x_i {}^o G_i(T) \tag{2}$$

Here x_i is the mole fraction of component i and ${}^oG_i(T)$ is the free energy of that component relative to its standard state-typically the most stable form at 298.15 K. The second term in equation (1) is the ideal entropy of mixing:

$$S_m = \sum_{s=1}^{m} a^s \sum_{i=1}^{n} y_i \ln y_i \tag{3}$$

Here a^s is the number of sites on the sublattice s and y_i is the site fraction of each component on the particular sublattice. Finally the third term is excess free energy which is composed of interaction parameters among different components within the same sublattice. The excess free energy is also summed over m sublattices. Interaction terms between sublattices are also included. The excess free energy can be expressed with a variety of polynomials, but typically for alloys, a Redlich-Kister polynomial (refs. 9 and 10) is used:

$${}^E G_m = u_i y_j \sum_{k=0}^{n} {}^k L_{ij}^M \left(y_i - y_j\right)^k \tag{4}$$

TABLE II.—COMPOSITIONS OF THE ALLOYS IN ATOMIC PERCENT STUDIED BY RITZERT et al. (refs. 1 and 2).

Alloy	Al	Co	Cr	Mo	Ni	Re	Ta	W
1	13.18	12.71	4.56	0.78	62.41	1.84	2.48	2.04
2	11.90	12.92	4.48	0.79	63.47	1.86	2.54	2.05
3	12.58	12.80	4.47	0.79	62.96	1.86	2.50	2.05
4	14.48	10.91	3.64	0.33	63.35	1.90	2.96	2.43
5	12.66	16.73	3.59	1.34	58.08	2.11	2.99	2.49
6	12.47	16.48	3.66	1.32	59.27	1.91	2.95	1.93
7	14.19	16.57	3.68	1.33	57.73	2.09	2.47	1.94
8	14.09	16.45	6.09	0.33	55.58	2.08	2.94	2.45
9	12.69	10.97	6.10	1.32	62.09	1.91	2.45	2.48
10	14.03	10.92	6.07	1.32	60.72	2.07	2.93	1.96
11	12.39	11.13	3.71	1.34	63.96	1.93	3.02	2.52
12	12.95	12.60	4.44	0.85	62.91	1.81	2.48	1.97
13	12.85	12.61	4.52	0.77	62.97	1.80	2.50	1.99
14	13.38	12.57	4.55	0.78	62.47	1.81	2.48	1.96
15	13.06	10.79	3.63	0.33	65.40	2.03	2.40	2.36
16	14.22	15.26	5.56	1.18	56.89	1.86	2.75	2.29
17	14.86	16.16	3.61	1.31	57.30	2.02	2.87	1.87
18	12.93	15.96	5.99	1.30	57.74	1.84	2.38	1.86
19	13.32	16.26	6.06	1.31	56.27	2.00	2.89	1.89
20	14.68	10.61	6.07	0.39	61.70	1.83	2.36	2.36
21	14.75	15.93	3.59	0.32	58.90	1.80	2.37	2.33
22	14.46	10.61	3.57	1.29	64.05	1.80	2.36	1.85
23	12.76	12.75	4.70	0.78	62.60	1.85	2.53	2.04
24	12.77	12.86	4.58	0.78	62.65	1.85	2.49	2.01
25	12.98	12.73	4.69	0.78	62.41	1.85	2.52	2.04
26	12.92	10.97	6.22	0.33	62.30	1.91	2.94	2.41
27	13.03	10.86	3.74	1.31	64.69	2.06	2.43	1.88
28	13.02	16.18	6.15	0.33	57.61	1.89	2.43	2.39
29	13.09	10.92	3.76	0.33	65.02	2.07	2.93	1.89
30	14.70	10.90	3.75	1.31	62.41	2.06	2.44	2.43
31	13.07	11.10	6.29	1.34	60.62	2.10	3.01	2.48
32	12.43	10.85	3.70	0.32	66.53	1.87	2.40	1.89
33	14.70	16.09	6.20	0.32	56.06	1.83	2.91	1.89
34	12.98	12.84	4.69	0.78	62.31	1.85	2.52	2.04
35	12.98	12.84	4.69	0.78	62.31	1.85	2.52	2.04
36	12.97	16.52	3.79	0.33	58.98	1.95	2.99	2.46
37	12.91	10.76	6.22	0.32	63.45	2.04	2.41	1.89
38	12.94	16.48	6.23	1.32	56.01	2.11	2.46	2.45
39	12.53	16.26	3.73	0.33	60.80	2.05	2.42	1.87
40	13.05	16.33	6.17	0.33	57.22	2.06	2.92	1.92
41	14.68	10.81	3.69	0.32	64.19	2.03	2.39	1.88
42	12.71	16.49	3.79	1.32	58.87	1.91	2.46	2.45
43	13.11	10.93	6.20	1.32	61.66	1.90	2.97	1.92
44	14.57	16.46	3.78	0.33	57.36	2.08	2.98	2.45

TABLE III.—ELEMENTS AND PHASES IN MOST RECENT VERSION OF NI-DATABASE

Elements in Ni-alloy database	Ni, Al, Co, Cr, Hf, Mo, Nb, Ta, Ti, W, Zr, B, C, Re
Phases in Ni-alloy database	Liquid, γ, γ', η, Ni_3Nb, σ, μ, Laves, MC, $M_{23}C_6$, M_6C, M_7C_3, M_3B_2, MB_2, α(Cr, Mo, W), P, R

Here ${}^{k}L_{ij}^{M}$ is the interaction coefficient. These coefficients are determined by fitting to experimental data. Database development is a long and arduous task, involving collection and fitting of large datasets. Multicomponent databases are put together from well-assessed binaries and ternaries.

The heart of the ThermoCalc code is a free energy minimizer. Given a series of constraints—temperature, pressure, and amounts of components—the free energy of the system is minimized and the phase composition is determined for these conditions. This is the first step in a ThermoCalc calculation and provides information on phases present and their elemental composition. Using this single equilibria as a starting point, property diagrams (stepping one variable and recording property changes) or a phase diagram (mapping of composition and temperature) can be determined.

ThermoCalc allows calculation of a variety of thermodynamic information for the complex, multicomponent system of Ritzert et al. (refs. 1 and 2). Perhaps the most relevant is the phase fraction at a given temperature for a given composition. This can be directly compared to the data of Ritzert et al. (refs. 1 and 2). Multicomponent phase diagrams are best presented as phase fraction diagrams with the composition fixed and the temperature varying. From this type of diagram solvus temperatures for the TCP phases can be determined. In addition, isopleths at a constant temperature with one component varying over a small range illustrate the effect of that particular element on the formation of TCP phases.

PHASE VOLUME FRACTIONS AT 1366 K (1093 °C)

As noted, the alloys of Ritzert et al. (refs. 1 and 2) were heat treated at 1366 K for 400 hrs. This very likely allows equilibration of the alloys and thus provides good points for comparison to equilibrium thermodynamic calculations. For the Ni-database, ThermoCalc gives an output in terms of mole fraction or weight fraction of each phase. The composition and the molecular weight of each phase is also given. Experimental measurements are in volume fraction of each phase. In order to convert the calculated mole fraction to volume fraction, a molar density for each phase is required:

- γ The average lattice parameter of 0.352 nm and four atoms per fcc unit cell were used to calculate a molar density of 0.1523 mole/cc.
- γ' The lattice parameters were experimentally measured for each of the forty-four alloys (ref. 11) and are given in Appendix A. Four atoms per unit cell were used to calculate the molar density for each alloy.
- P Phase The lattice parameters were measured for the alloys (ref. 11) with a larger amount of TCP phase, detectable by XRD. They are listed in the Appendix. The orthorhombic unit cell was used with 56 atoms per unit cell to calculate the molar density. When the lattice parameter was not experimentally measured, the lattice parameters in table I were used to calculate a molar density.
- μ Phase The lattice parameters in table I were used. The hexagonal unit cell was used with 39 atoms per unit cell to calculate a molar density.

Table IV lists the calculated volume fraction of all phases predicted at 1366 K for each of the forty four alloys. The shaded rows are the alloys for which TCP phases are predicted to form. These data are shown in graphical form in figures 1(a) to (c). The calculations tend to over-predict the volume fraction of γ; under-predict the volume fraction of γ', and under-predict the volume fraction of TCP phase.

Generally when the volume fraction of TCP is greater than about 0.02, its formation is predicted. The only exception is alloy 42, where a very small amount of TCP is observed (volume fraction = 0.0056) and μ phase formation is predicted. For the other alloys, the volume percent of TCP predicted is too low—generally by a factor of 2 to 8.

TABLE IV.—CALCULATED VOLUME PERCENT OF THE PREDICTED PHASES AND MEASURED VOLUME PERCENT OF TCP PHASE AT 1366 K.
[Shaded rows are alloys for which TCP was predicted from the calculations.]

Alloy	Calculated Volume Fractions					Measured Volume Fraction		
	γ	γ'	P	μ	σ	γ	γ'	TCP
1	0.5278	0.4722				0.3787	0.6171	0.0042
2	0.6222	0.3778				0.3940	0.6037	0.0023
3	0.5723	0.4277				0.4037	0.5952	0.0011
4	0.3504	0.6329	0.0167			0.3248	0.6305	0.0447
5	0.5501	0.4326	0.0173			0.4484	0.4960	0.0556
6	0.5339	0.4661				0.3816	0.6126	0.0058
7	0.4415	0.547	0.0115			0.4198	0.4945	0.0857
8	0.3763	0.5911	0.0326			0.3095	0.5680	0.1225
9	0.5307	0.4478	0.0139	0.0075		0.4510	0.4692	0.0798
10	0.3557	0.5988	0.0455			0.3120	0.5546	0.1334
11	0.5685	0.4208		0.0107		0.4132	0.5422	0.0446
12	0.6013	0.3987				0.3587	0.6389	0.0024
13	0.5504	0.4496				0.3705	0.6265	0.003
14	0.5106	0.4894				0.3856	0.6111	0.0033
15	0.5432	0.4568				0.4321	0.5650	0.0029
16	0.3648	0.5979	0.0373			0.3350	0.4980	0.167
17	0.3266	0.6464	0.027			0.2954	0.6136	0.091
18	0.5526	0.4458	0.0016			0.5075	0.4688	0.0238
19	0.5108	0.4652	0.024			0.4318	0.4886	0.0796
20	0.3847	0.5966	0.0187			0.4059	0.5050	0.0891
21	0.4174	0.5826				0.3476	0.6354	0.017
22	0.4307	0.4657	0.0036			0.4025	0.5481	0.0494
23	0.4275	0.5725				0.3431	0.6523	0.0046
24	0.5591	0.4409				0.3994	0.5992	0.0014
25	0.5377	0.4623				0.3388	0.6592	0.002
26	0.4795	0.5086	0.0119			0.4481	0.5288	0.0231
27	0.547	0.453				0.4226	0.5719	0.0055
28	0.5407	0.4593				0.4532	0.5362	0.0106
29	0.4989	0.5011				0.4089	0.5908	0.0003
30	0.3475	0.6176	0.0266	0.0083		0.3288	0.6062	0.065
31	0.4807	0.4775	0.0418			0.3836	0.5064	0.11
32	0.6118	0.3882				0.4777	0.5223	0
33	0.3698	0.6159	0.0143			0.3590	0.5962	0.0448
34	0.5384	0.4616				0.3775	0.6205	0.002
35	0.5382	0.4618				0.3629	0.6339	0.0032
36	0.4872	0.5128				0.3810	0.6116	0.0074
37	0.5626	0.4374				0.4463	0.5471	0.0066
38	0.4972	0.4698	0.0175	0.0154		0.4195	0.5089	0.0716
39	0.6024	0.3976				0.4588	0.5412	0
40	0.5025	0.4975				0.4285	0.5600	0.0115
41	0.4302	0.5698				0.3796	0.6151	0.0053
42	0.5565	0.4404		0.0031		0.4512	0.5432	0.0056
43	0.4454	0.53	0.0246			0.4395	0.4826	0.0779
44	0.3533	0.3627	0.0046	0.0151		0.2645	0.6806	0.0549

TABLE V.—MASS BALANCE FOR HIGH TCP PHASE ALLOYS

Alloy	Volume percent, TCP	Volume percent, γ	Volume percent, γ′	Total moles	Atomic percent, TCP	Atomic percent, γ	Atomic percent, γ′	Atomic percent, Re in, alloy	Atomic percent, Re in, γ	Atomic percent, Re left for TCP	Atomic percent, Re in TCP	Atomic percent, max TCP
16	16.7	36.48	59.79	16.330726	12.598582	34.021169	53.380247	1.86	2	1.179576	15.7	7.513226
8	12.25	37.63	59.11	15.858487	9.5166707	36.138687	54.344642	2.08	1.6	1.501781	20.21	7.430880
10	13.34	35.57	59.88	15.791303	10.407551	34.305661	55.286786	2.07	1.6	1.521109	19.44	7.824636
31	11	48.07	47.75	15.638211	8.6659529	46.815207	44.518839	2.1	n/d*			
5	5.56	55.01	43.26	15.370323	4.4565881	54.507787	41.035624	2.11	2.5	0.747305	22.23	3.361697
7	8.57	44.15	54.7	15.755129	6.7014621	42.678450	50.620086	2.09	1.6	1.407144	20.84	6.752134
9	7.98	53.07	44.78	15.594621	6.3043276	51.829159	41.866512	1.91	2	0.873416	20.74	4.211267
17	9.1	32.66	64.64	15.51975	7.2238277	32.050245	60.725926	2.02	2	1.378995	22.77	6.056192
19	7.96	51.08	46.52	15.542772	6.3095051	50.052101	43.638393	2	1.9	1.049010	20.07	5.226756
20	8.91	38.47	59.66	15.655121	7.0118397	37.425331	55.562828	1.83	1.7	1.193769	21.54	5.542104

*Not determined.

The high volume fraction (>0.05) found in many of these alloys was surprising. Table V is a mass balance to determine if this is reasonable. First the volume fractions are all converted to atom fractions. Then the amount of Re in the γ phase is removed from the total. From the remaining, the maximum possible atom fraction of TCP is estimated. The atom fractions of TCP less than about 0.08 are all reasonable. However the three alloys with atom fractions >0.09 do not seem consistent with a mass balance. The reasons for this are not clear and more microstructural work is underway to understand this.

Ritzert et al. (ref. 1) generated an empirical equation which predicts the volume fraction of TCP phases from mole fraction of Al, Cr, Mo, Re, Ta, W, and Co. Their equation also includes interaction terms: x(Al)*x(Co), x(Al)*x(Cr), x(Al)*x(Mo), x(Co)*x(Re), x(Cr)*x(Mo), x(Re)*x(W), and x(Ta)*x(W). In order to graphically illustrate some of their predictions and the particular effect of several elements, they present a series of response surfaces, which are given in figures 2(a) to (f). These are determined while setting the other element levels to their average values. Figure 2 shows that Co and Re have a mild interactive effect on TCP phase formation. At low Mo levels, Cr has little effect; however at high Mo levels Cr clearly leads to TCP phases. Cr and Al exhibit the strongest synergistic effect toward TCP formation. Similar conclusions can be drawn from the other response surfaces in figure 2.

These response surfaces can be generated from ThermoCalc by using the stepping option. Of the two components to be varied, one is held constant while the second is stepped. Then the first is incremented one notch and the second is stepped again. This procedure generates grids similar to those shown in figure 2. The results for each of the combinations shown in figure 2 are illustrated in figures 3(a) to (f). As seen in table IV, the volume fractions are lower than those measured. However, also as seen in table IV, the general trends in the experiments are reproduced from the phase calculations. Figure 3(a) is similar to figure 2(a) in showing the mild effect of Co and Re on TCP phase formation. Figure 3(b) shows that Mo and Cr together at levels above about x(Mo) = 0.011 and x(Cr) = 0.055 leads to TCP phase formation, as shown in figure 2(b). Figure 3(c) shows the strong interactive effect of Cr and Al at levels above about x(Cr) = 0.05 and x(Al) = 0.135, as observed in figure 2(c). Figure 3(d) is similar to figure 2(d) for x(Al) greater than about 0.135, TCP phase formation occurs for $0.11 < x(Co) < 0.16$. Figure 3(e) shows that increased W and Ta promote TCP phase formation, as does figure 2(e). However the effect is more pronounced in the calculations. Similarly the calculations show that W and Re tend to promote TCP formation (figs. 2(f) and 3(f)) with the effect being more pronounced in the calculations.

PARTITIONING OF ELEMENTS IN DIFFERENT PHASES

As discussed, ThermoCalc also gives the composition of each phase and thus partitioning of elements between phases can be readily determined. Ritzert (ref. 11) has done extensive analyses of the phase compositions within grains and at grain boundaries for 26 of the 44 alloys. Appendix B is the a listing of the measured and calculated compositions for γ, γ', and P phase within grains and at grain boundaries. The shaded rows are for the calculated compositions.

These data from appendix B are plotted in figures 4(a) to (g), 5(a) to (g), and 6(e) and (f) to graphically shown the variation from the predicted values. The experimental measurements in the grains and at the grain boundaries are averaged for these graphs. These data are summarized as follows:

1. γ Phase

   γ—Co-Calculations show good agreement with experimental measurements.

   γ—Mo-Calculations show good agreement with experimental measurements.

   γ—W-Calculations over-predict x(W) by about 0.006

   γ—Re-Calculations over-predict x(Re) by about 0.008

   γ—Ta-Calculations under-predict x(Ta) by about 0.005

   γ—Al-Calculations show reasonable agreement with x(Al).

   γ—Cr-Calculations show good agreement with experimental measurements

2. γ' Phase

   γ'—Co-Calculations under-predict x(Co) by about 0.02

   γ'—Mo-Calculations under-predict x(Mo) by about 0.002

   γ'—W-Calculations under-predict x(W) by about 0.004

   γ'—Re-Calculations do not predict changes in x(Re)

   γ'—Ta-Calculations over-predict x(Ta) by about 0.005

   γ'—Al-Calculations under-predict x(Al) by about 0.02 and do not predict changes in x(Al).

   γ'—Cr-Calculations under-predict x(Cr) by about 0.015

3. TCP Phase-P + μ Phases

   TCP-Ni-Calculations under-predict x(Ni) by about 0.2 and do not really predict changes in x(Ni).

   TCP-Co-Calculations under-predict x(Co) by about 0.07

   TCP-Mo-Calculations over-predict x(Mo) by about 0.05

   TCP-W-Calculations over-predict x(W) by about 0.05

   TCP-Re—Calculations over-predict x(Re) by about 0.05

   TCP-Cr-Calculations show good agreement with experimental measurements.

   TCP-Ta, Al-Predicted to be zero, but observed experimentally in TCP phases.

Several of these observations should be discussed further. The calculated compositions of the γ and γ' phases show reasonable agreement with the measured values. Where differences are noted, they tend to be small. The differences between the calculated TCP compositions and the measured values are more significant. As indicated, the predicted TCP phase was generally P phase. This is a complex phase and the mathematical description of it in the Ni-database may not be entirely accurate. The calculations showed no Ta or Al in this phase, which was in conflict with the experimental measurements. The calculations under-predicted Ni in this phase. However the problem here may be partially in the experimental measurement. Some of the γ and/or γ' phase may have also been sampled. Clearly a refinement of the models and model parameter are required to more accurately predict TCP phase formation in this composition range. More experimental studies on the individual TCP phases would assist in developing these model parameters.

TABLE VI. LIQUIDUS, SOLIDUS, AND γ' SOLVUS TEMPERATURES (K)

Alloy	Measured liquidus	Calculated liquidus	Measured solidus	Calculated solidus	Measured γ' solvus	Calculated γ' solvus
1	1699	1680	1658	1625	1544	1600
2	1697		1652		1556	
3	1698		1661		1513	
4	1697	1674	1664	1623	1583	1628
5	1684	1674	1644	1609	1536	1609
6	1697	1676	1649	1612	1553	1612
7	1679	1673	1626	1610	1535	1612
8	1675	1657	1628	1592	1553	1600
9	1686	1672	1642	1619	1537	1564
10	1670	1658	1619	1598	1559	1600
11	1685	1679	1648	1626	1555	1597
12	1707	1682	1658	1629	1553	1594
13	1711		1676		1554	
14	1697		1657		1553	
15	1721	1693	1677	1643	1567	1596
16	1667	1655	1616	1593	1561	1599
17	1683	1662	1638	1604	1579	1613
18	1681	1668	1645	1606	1523	1582
19	1678	1658	1633	1591	1536	1595
20	1692	1666	1645	1609	1571	1610
21	1694	1676	1643	1620	1571	1623
22	1692	1678	1653	1625	1579	1625
23	1698	1681	1653	1627	1550	1590
24	1697	1669	1664	1613	1556	1598
25	1702		1658		1554	
26	1690		1653		1576	
27	1705	1687	1671	1636	1562	1587
28	1693	1672	1656	1608	1534	1594
29	1700	1686	1667	1632	1581	1622
30	1675	1674	1642	1618	1580	1619
31	1670	1660	1631	1600	1564	1587
32	1699	1696	1674	1650	1552	1576
33	1676	1653	1633	1593	1569	1602
34	1695	1680	1659	1625	1548	1596
35	1692		1658		1551	
36	1689	1678	1656	1617	1561	1619
37	1698	1680	1655	1628	1544	1576
38	1679	1664	1643	1597	1521	1580
39	1704	1693	1667	1635	1532	1591
40	1681	1667	1644	1601	1539	1603
41	1699	1684	1656	1630	1588	1631
42	1692	1679	1657	1619	1539	1593
43	1682	1662	1641	1604	1559	1594
44	1680	1667	1637	1610	1582	1618

TABLE VII.—CALCULATED SOLVUS

Alloy	σ phase	P phase	μ phase
1	1034	1314	1205
2			
3			
4	1192	1442	1279
5	807		1439
6	821		1322
7	969	1409	1284
8	1253	1496	1301
9	1072	1426	1438
10	1144	1497	1162
11	823		1412
12	987	1287	1175
13			
14			
15	1149	1256	1209
16	1152	1487	1488
17	1031	1463	1275
18	1074	1372	1271
19	1128	1451	1260
20	1266	1461	1230
21	1088		1354
22	915	1381	1111
23	1023	1296	1210
24			
25			
26	1237	1423	1254
27	825	1337	1065
28	1161		1367
29	1176	1259	1041
30	1011	1433	1495
31	1142	1507	1306
32	1078		718
33	1290	1439	1244
34	1036	1311	1213
35			
36	955		1345
37	1290	1308	973
38	1094	1454	1467
39	1017		1099
40	1227	1365	1221
41	1240	1319	852
42	793		1378
43	1111	1448	1202
44	1164	1428	1465

TABLE VIII.—AVERAGE ALLOY COMPOSITION

Element	Average amount (mole fraction)
Al	0.1334
Co	0.1343
Cr	0.0474
Mo	0.0082
Ni	0.6092
Re	0.0194
Ta	0.0264
W	0.0213

PHASE FRACTION DIAGRAMS, LIQUIDUS, SOLIDUS, AND SOLVUS TEMPERATURES

Phase fraction diagrams are a convenient way to display data for multi-component alloys. These type of diagrams show just that—the mole fraction of each phase at a particular temperature. Phase fraction diagrams for 37 compositions are given in appendix C. From the tabulated values which produce these diagrams, the liquidus, solidus, and solvus temperatures can be determined. These were also measured experimentally via Differential Thermal Analysis (DTA) (ref. 11). Table VI lists the measured and calculated liquidus, solidus and γ' solvus temperatures. For easier comparison, these are plotted in figures 7(a) to (c). Note that the measured liquidus temperatures are about 20° higher than those calculated, the measured solidus temperatures are about 40° higher than those calculated, and the measured γ' solvus temperatures are about 40° lower than those calculated.

The TCP phase solvus temperatures were not measured. Table VII lists the calculated solvus temperatures for σ, P, and μ phases. Note that the solvus temperatures for σ phase are generally lowest, indicating the equilibrium TCP phases after the 1366 K heat treatment are P and μ.

ISOPLETHS

A second way to display the phases in a multicomponent system is with an isoplethal section. An isopleth for a three component system is illustrated in Figure 8 (ref. 12). This is simply a vertical cut and creates a diagram with the appearance of a simple binary. However, since this is a multicomponent diagram, tie lines cannot be drawn in the plane of the isopleth and no phase fractions can be determined from the diagrams. The boundary lines are often termed "zero phase fraction" lines and determine when a particular phase appears or disappears. Thus the diagrams simply show what phases are stable at a particular temperature and composition. The average alloy composition is given in table VIII.

Seven isopleths were calculated by varying each element in a sufficient range to put the studied compositions in the middle of the diagram. These are shown in figures 9 to 15. These are useful in that they illustrate the effects of a particular alloying element on a particular phase as a function of temperature. Al, Cr, Co, Mo, Re, Ta, and W all have significant effects on forming TCP phases. Figure 16 is an isopleth at 1366 K showing the effect of varying Al and Cr.

SUMMARY AND CONCLUSIONS

Computational thermodynamics has been applied to a series of alloys based on the nickel-base superalloy René N6. The Ni superalloy database developed by Saunders (ref. 3) was used in conjunction with ThermoCalc (ref. 4) to model a series of forty-four alloys. Experimental data for phase volume fraction of TCP phases and partitioning of elements between γ, γ', and TCP phases have been compared to calculations. In general the calculations show the same general trends as the experimental results. However for many compositions, TCP phases form and are not predicted by ThermoCalc and the Ni superalloy database. Only when TCP forms at levels of greater than a volume fraction of 0.02 is it actually predicted. The calculated compositions of the γ and γ' phases show reasonable agreement with the measured values. The calculated compositions of the TCP phases do not agree with those measured. Clearly more modeling and experimental work are needed to refine the descriptions of these complex phases.

In addition, phase fraction diagrams and solvus temperatures were calculated for each of the compositions studied. These show that P and occasionally μ phase are the most important in the temperature regime studied. The σ phase is only important at lower temperatures. Isopleths were also constructed based on the average composition of the alloys studied. Seven isopleths were constructed, with small variations in Al, Co, Cr, Mo, Re, Ta, and W, respectively.

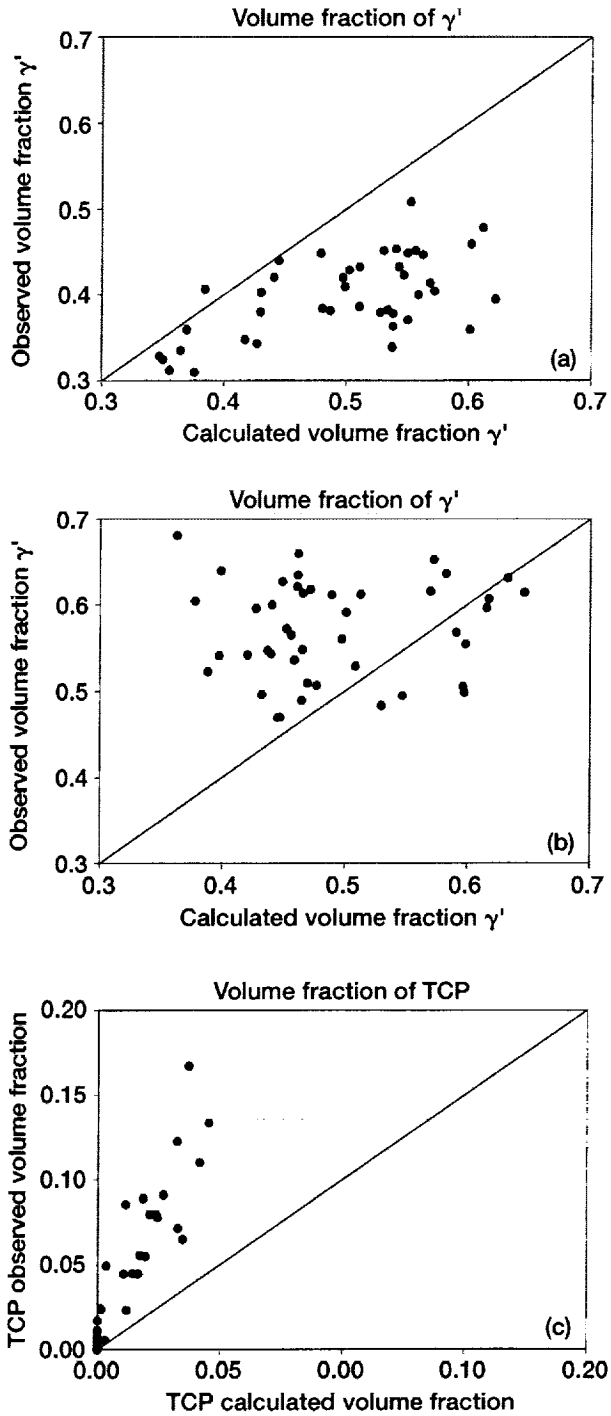

Figure 1.—Observed volume fraction verses measured volume fraction for (a) γ, (b) γ', and (c) TCP phases.

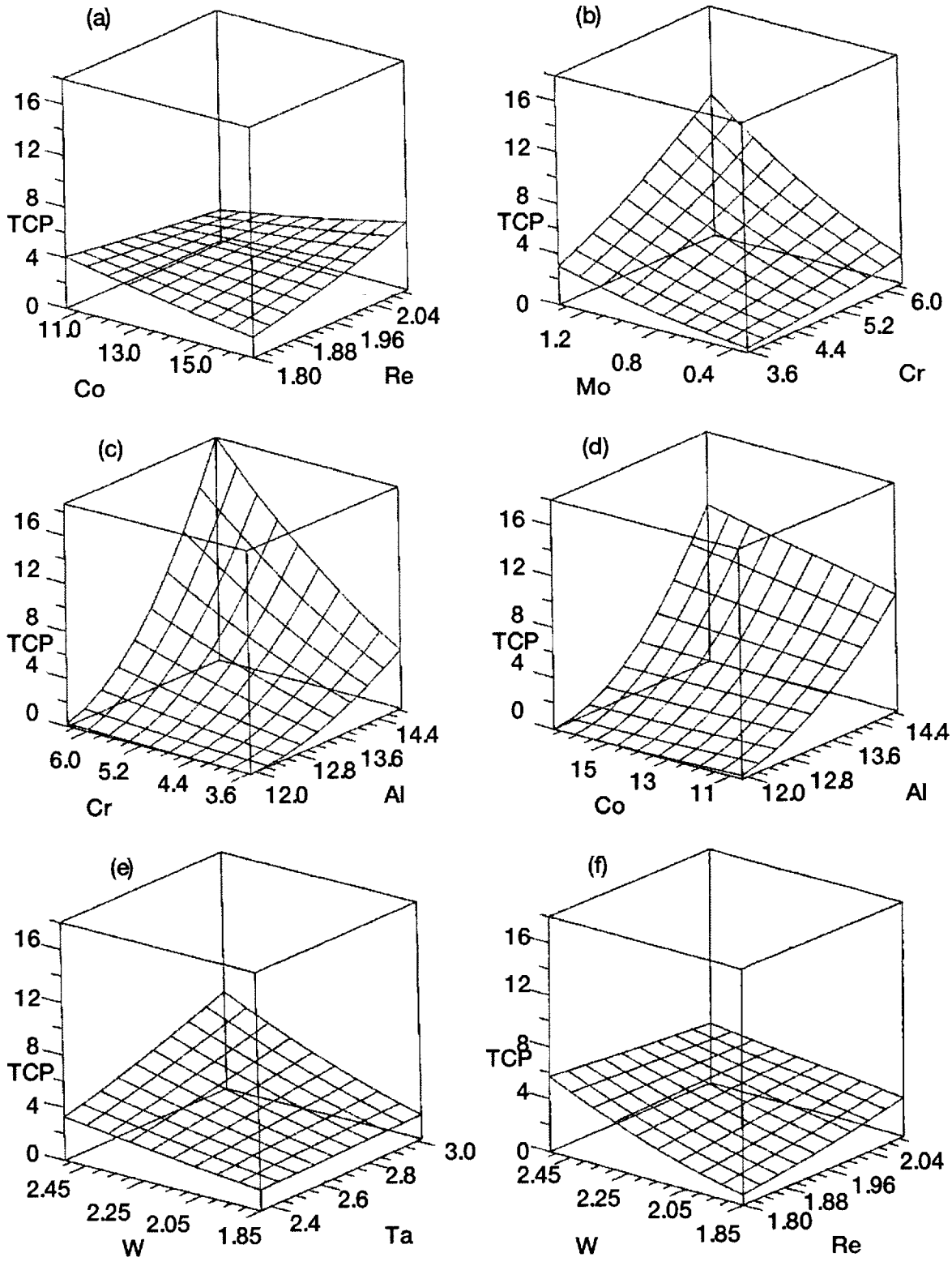

Figure 2.—Response surfaces from Ritzert et al. (1) showing effects of (a) Co Re, (b) Mo Co, (c) Al Cr, (d) Co Al, (e) W Ta, and (f) W Re. Compositions are in atomic percent.

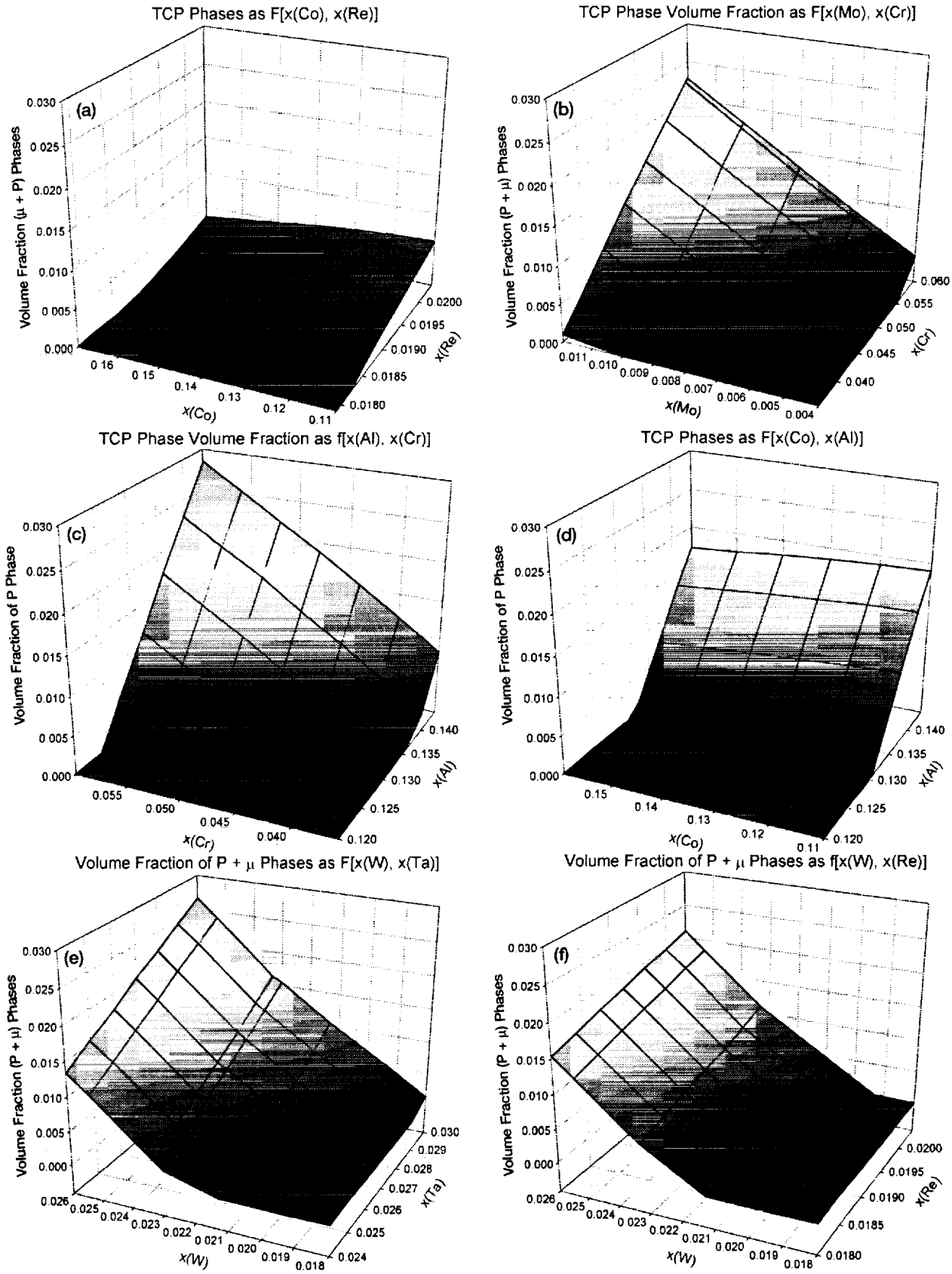

Figure 3.—Response surfaces calculated from the Saunders database (5) and ThermoCalc (6) showing effects of (a) Co Re, (b) Mo Co, (c) Al Cr, (d) Co Al, (e) W Ta, and (f) W Re.

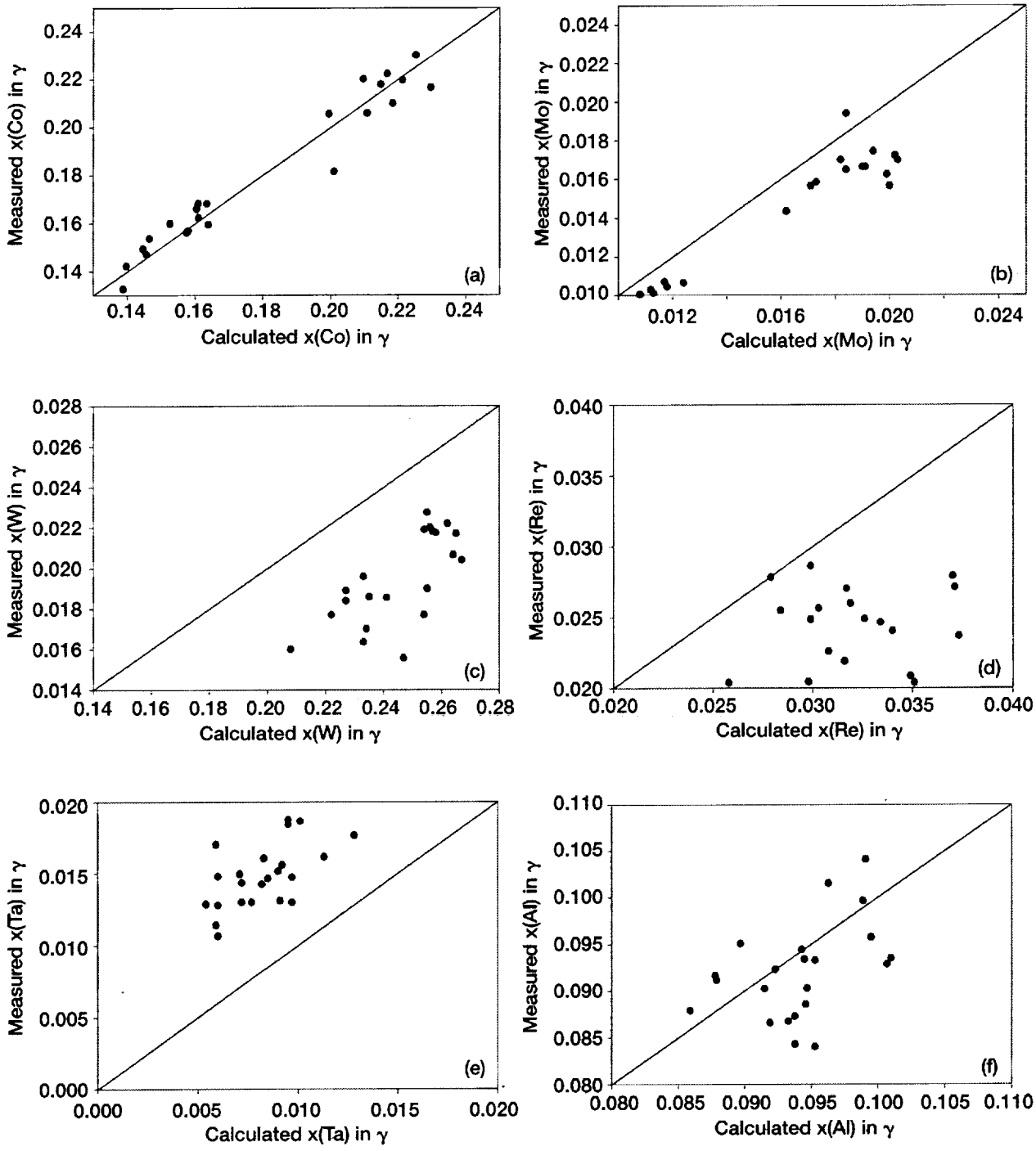

Figure 4.—Measured mole fraction verses calculated mole fraction in γ for (a) Co, (b) Mo, (c) W, (d) Re, (e) Ta, (f) Al, and (g) Cr.

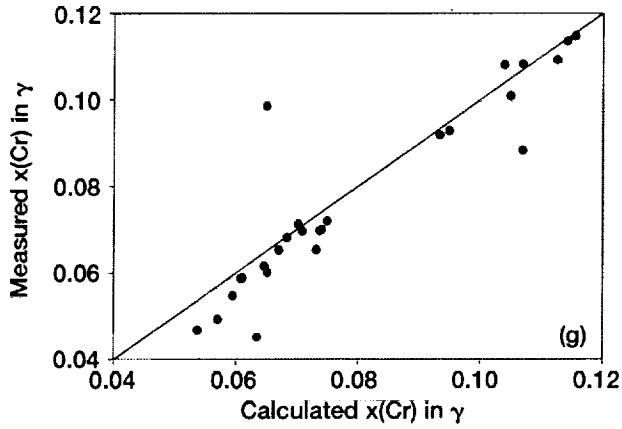

Figure 4.—Concluded. Measured mole fraction verses calculated mole fraction in γ for (g) Cr.

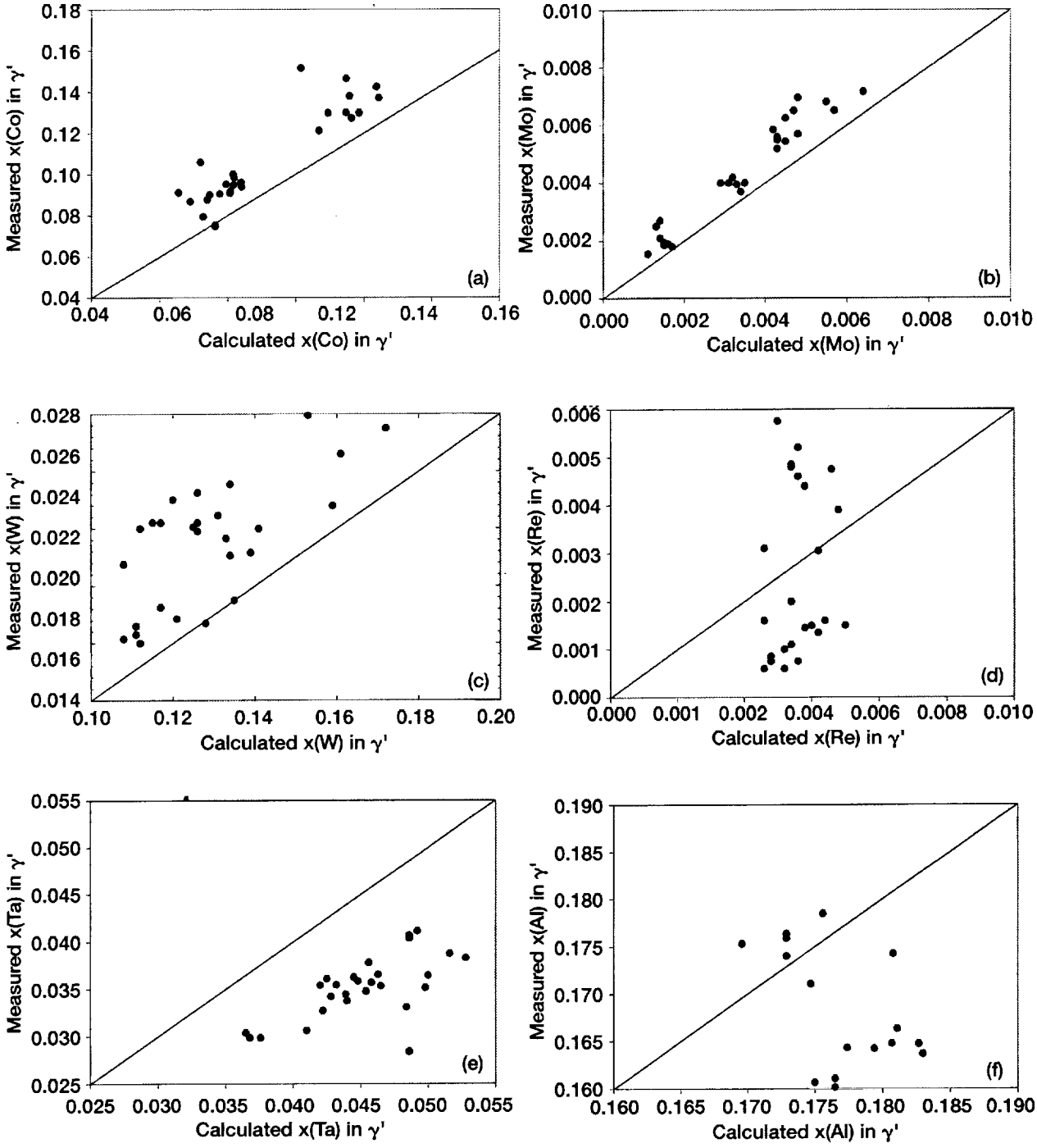

Figure 5.—Measured mole fraction verses calculated mole fraction in γ' for (a) Co, (b) Mo, (c) W, (d) Re, (e) Ta, (f) Al, and (g) Cr.

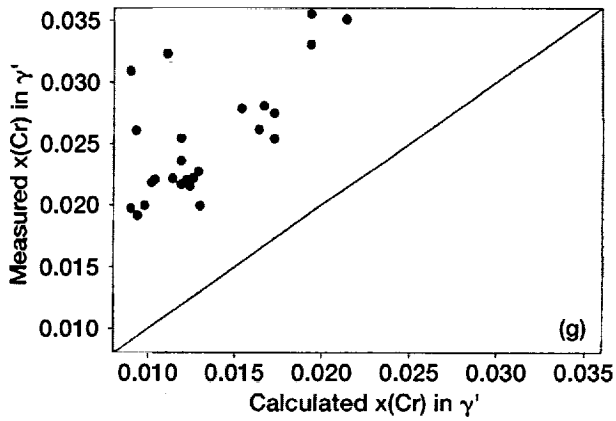

Figure 5.—Concluded. Measured mole fraction verses calculated mole fraction in γ' for (g) Cr.

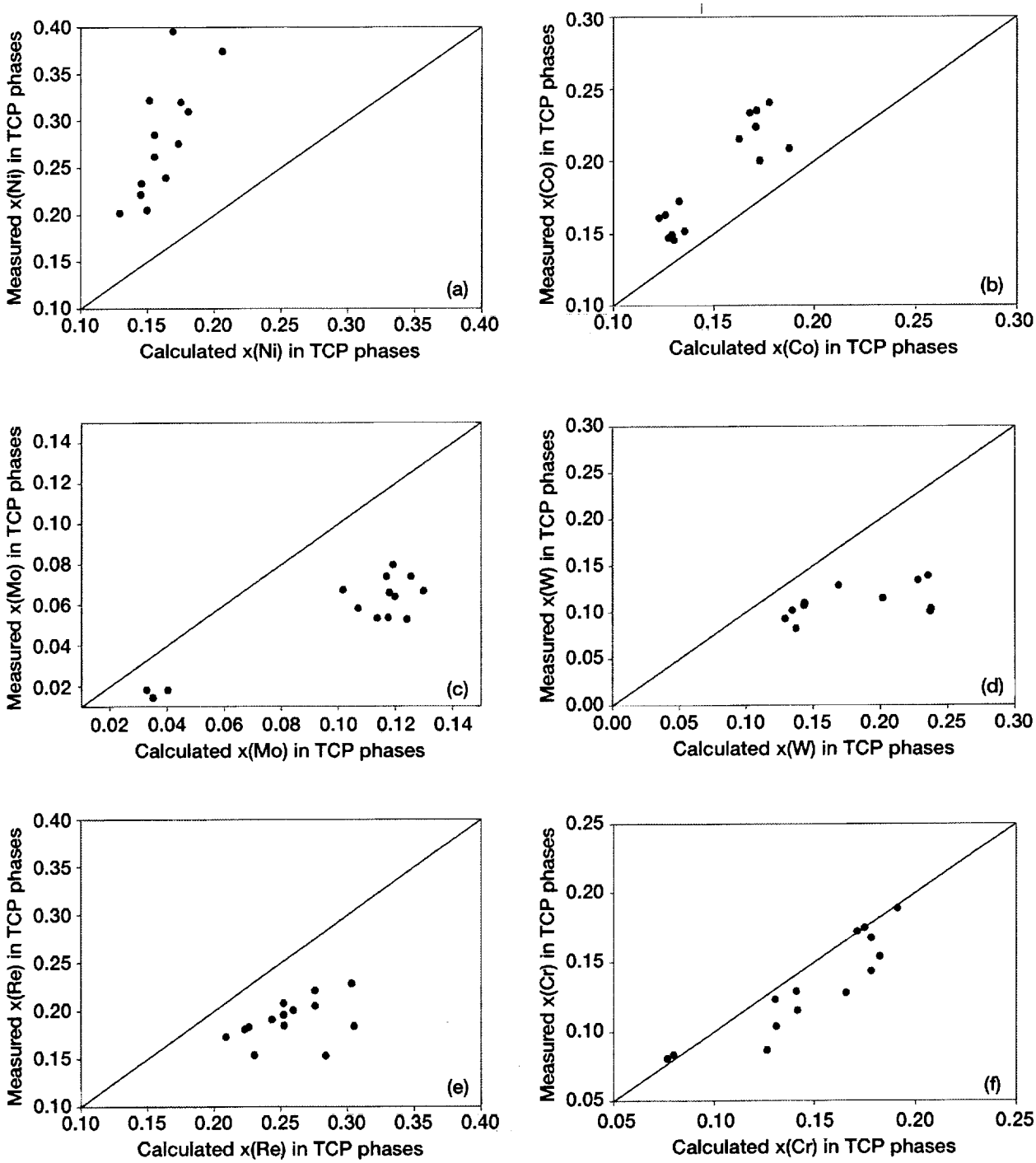

Figure 6.—Measured mole fraction verses calculated mole fraction in TCP phases for (a) Ni, (b) Co, (c) Mo, (d) W, (e) Re, and (f) Cr.

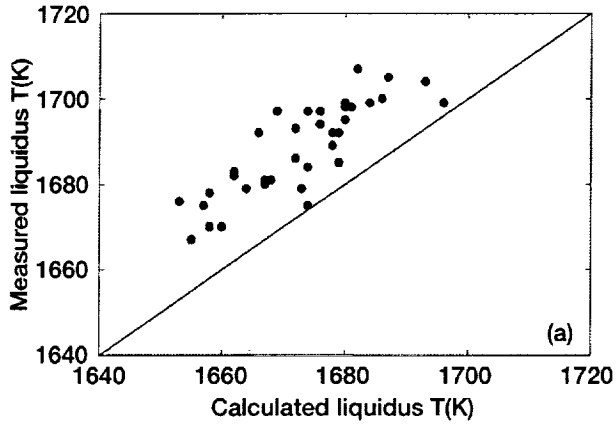

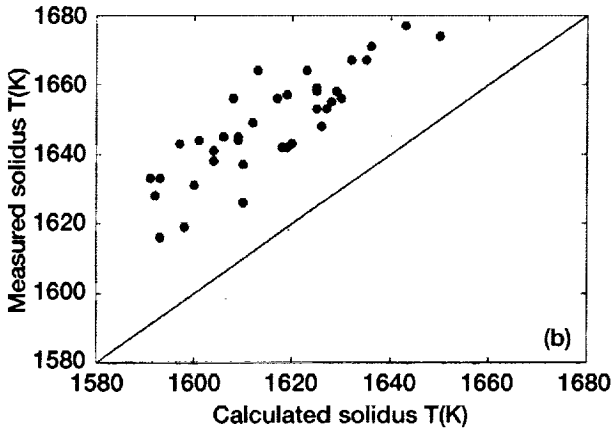

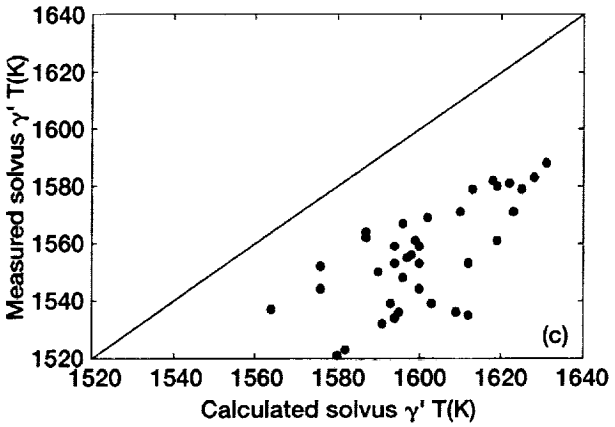

Figure 7.—Measured phase boundaries verses calculated values for (a) liquidus, (b) solidus, and (c) γ' solvus.

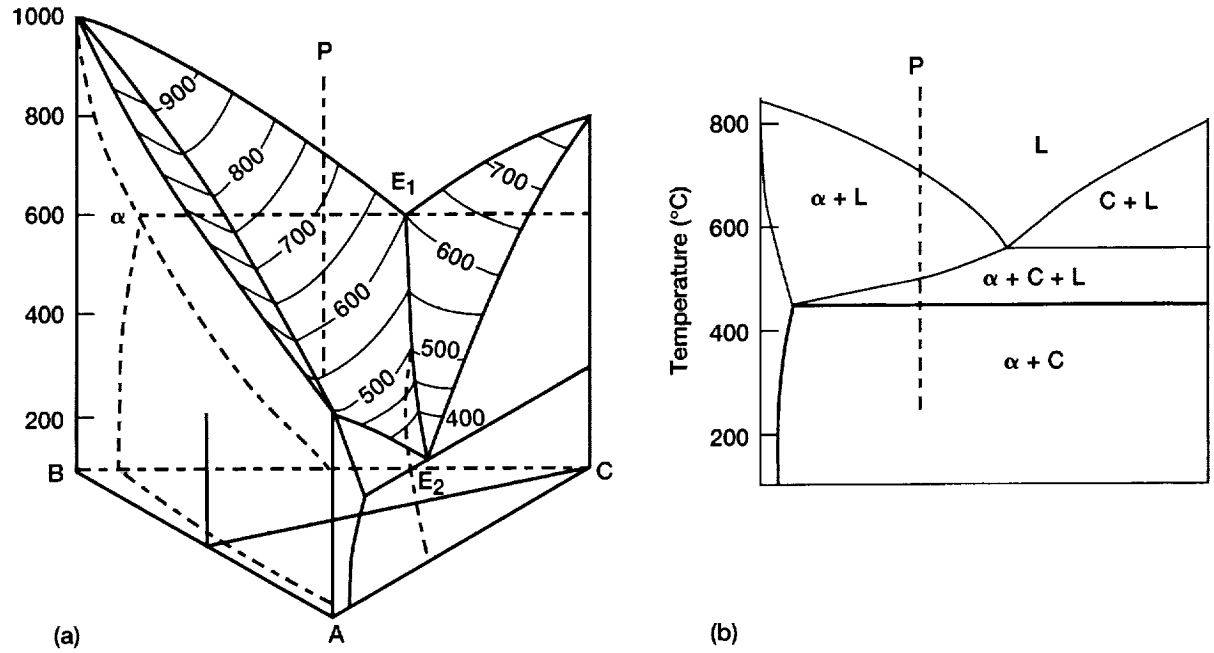

Figure 8.—Example of isopleth for a ternary system. Note that tie lines cannot be drawn in (b) as it is not a true binary. (a) Ternary system with solid solution. (b) Vertical section taken on a line C through P of system shown in (a). Adapted from reference (12).

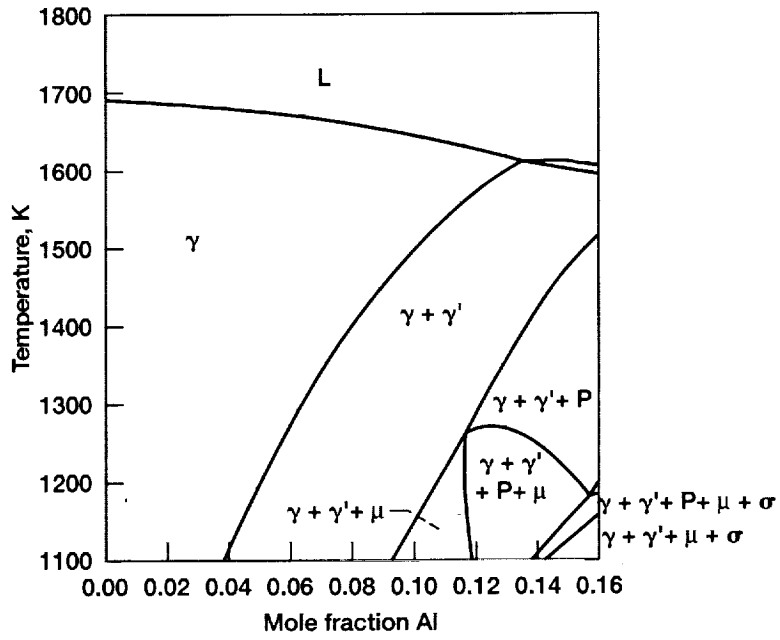

Figure 9.—Isopleth for Al.

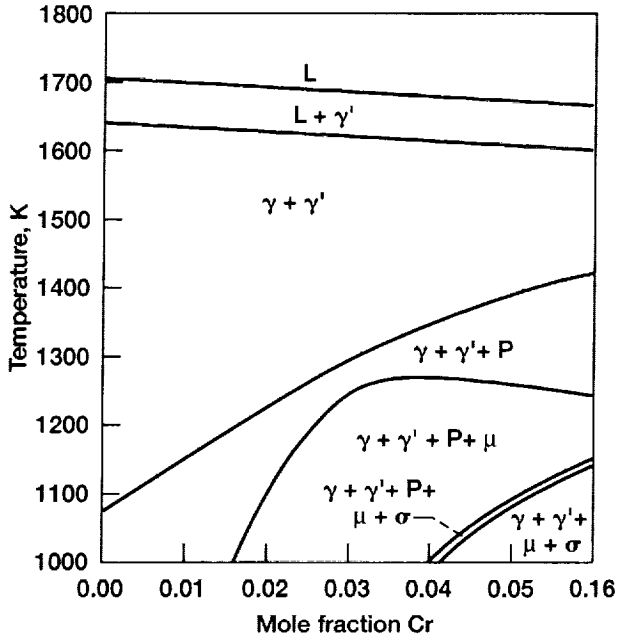

Figure 10.—Isopleth for Cr.

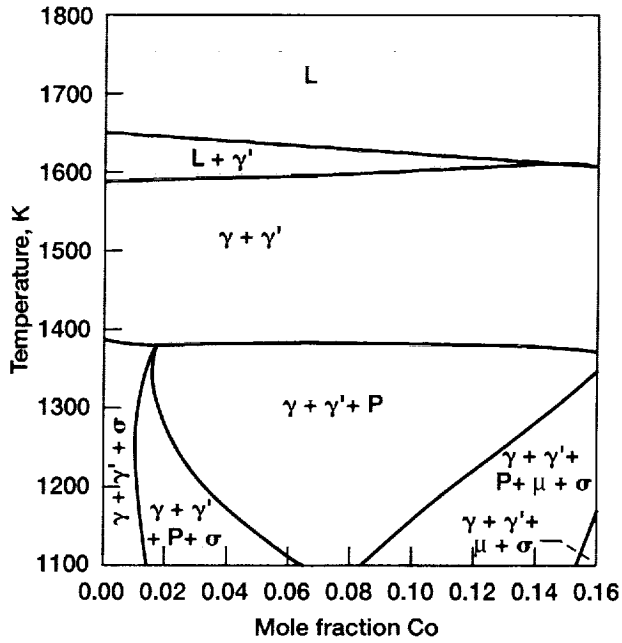

Figure 11.—Isopleth for Co.

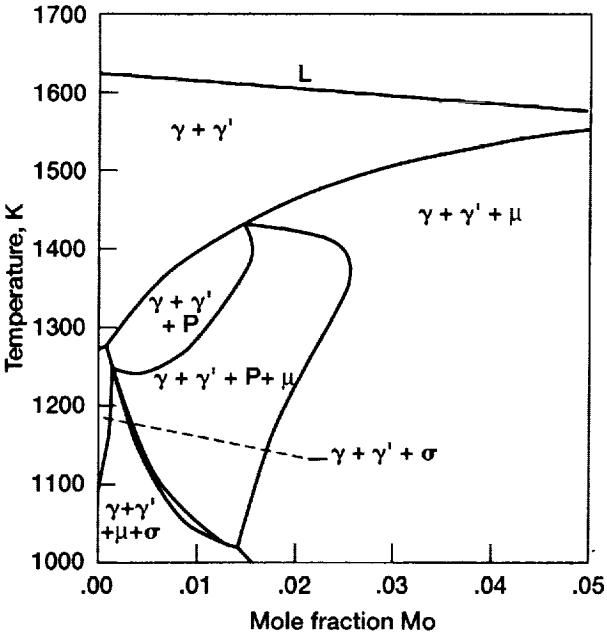

Figure 12.—Isopleth for Mo.

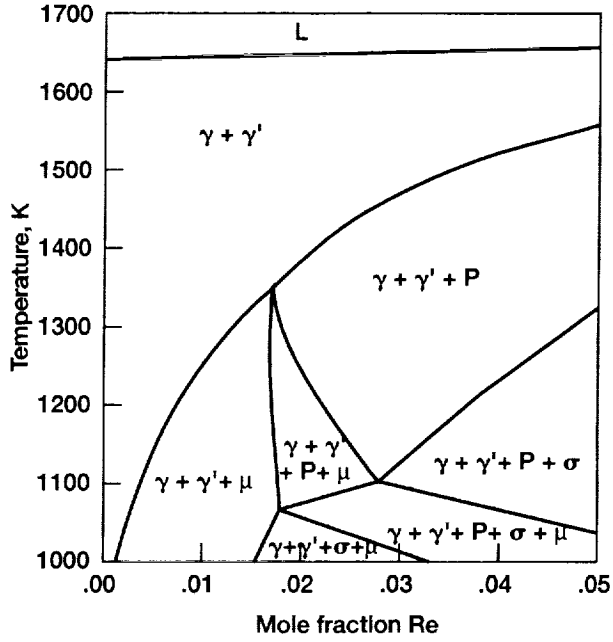

Figure 13.—Isopleth for Re.

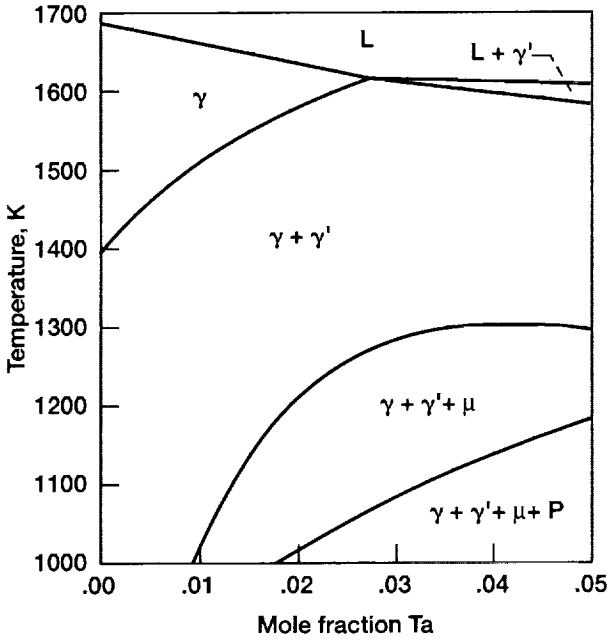

Figure 14.—Isopleth for Ta.

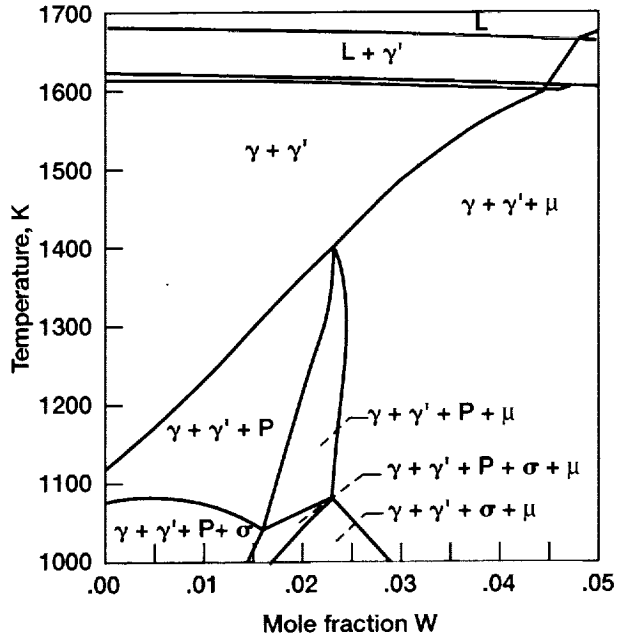

Figure 15.—Isopleth for W.

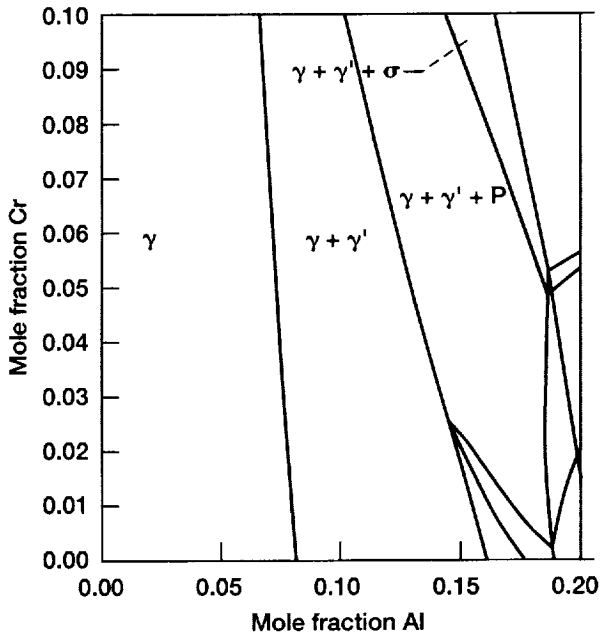

Figure 16.—Isopleth showing variation of Al and Cr at T = 1366 K.

APPENDIX A

TABLE A.1.—LATTICE PARAMETERS FOR γ'; AND P PHASE MEASURED BY RITZERT AND USED TO CALCULATE MOLAR DENSITIES (ref. 11)

Alloy	γ'	P phase lattice parameters		
	heat treat	a	b	c
1	3.573			
2	3.576			
3	3.577			
4	3.571	9.25	17.11	4.77
5	3.573	8.59	15.94	4.43
6	3.579	8.81	16.34	4.5
7	3.576	9.13	17.11	4.77
8	3.578	9.34	17.68	4.94
9	3.539	8.89	16.66	4.63
10	3.571	9.29	17.35	4.86
11	3.584	9.43	17.62	4.89
12	3.596			
13	3.584			
14	3.589			
15	3.588			
16	3.587	9.25	17.15	4.81
17	3.596	9.21	17.29	4.83
18	3.596	9.06	16.88	4.72
19	3.596	9.38	17.46	4.9
20	3.598	8.74	16.97	4.57
21	3.587			
22	3.565			
23	3.588			
24	3.577			
25	3.579	8.67	16.22	4.52
26	3.568	9.09	17.13	4.77
27	3.576	9.33	16.94	4.88
28	3.577			
29	3.58			
30	3.555			
31	3.568			
32	3.578			
33	3.577			
34	3.576			
35	3.577			
36	3.581			
37	3.577			
38	3.575			
39	3.576			
40	3.56			
41	3.575			
42	3.555			
43	3.578			
44	3.573			

APPENDIX B

Shaded rows are calculated values.

TABLE B.1(a).—TCP PHASE COMPOSITION AT GRAIN BOUNDARIES

Alloy	Nickel	Cobalt	Molybdenum	Tungsten	Rhenium	Tantalum	Aluminum	Chromium
1	25.23	18.40	4.18	11.88	26.80	1.59	0.44	11.49
2	24.92	18.22	4.12	12.04	27.75	1.67	0.37	10.90
3	23.42	18.32	4.24	11.92	28.53	1.49	0.21	11.88
4	24.99	18.09	2.14	14.32	26.72	1.58	0.08	12.07
P Phase	16.89	12.74	3.50	23.69	30.53	0.00	0.00	12.65
5	23.07	22.84	6.70	12.36	22.23	2.01	0.66	10.11
μ Phase	17.49	18.75	11.37	23.77	20.89	0.07	0.00	7.67
6	23.61	23.06	7.38	10.98	22.60	2.07	0.48	9.82
7	20.80	22.27	7.21	10.92	20.84	1.76	0.46	15.74
P Phase	15.14	17.29	12.41	13.73	28.38	0.00	0.00	13.05
8	19.87	23.44	1.86	13.96	20.21	2.77	0.22	17.68
P Phase	12.94	16.79	3.28	23.55	25.94	0.00	0.00	17.50
9	26.80	16.05	6.75	13.36	20.74	1.36	0.58	14.36
μ phase	20.18	13.35	10.95	23.35	20.66	0.04	0.00	11.47
P Phase	18.52	12.71	10.45	17.00	24.58	0.00	0.00	16.75
10	22.56	18.28	7.60	11.22	19.44	1.82	0.26	18.83
P Phase	16.36	13.28	11.69	14.34	25.22	0.00	0.00	19.11
11	28.25	17.60	6.84	12.61	22.37	1.58	0.77	9.98
	20.62	13.55	11.75	23.73	22.32	0.04	0.00	7.99
12	25.01	19.35	4.25	12.15	25.52	1.70	0.21	11.82
13	24.77	19.38	4.11	12.31	25.60	1.74	0.25	11.83
14	25.12	18.65	4.01	12.55	25.80	1.63	0.18	12.05
15	28.81	14.97	1.68	11.64	30.28	1.31	0.85	10.47
16	19.24	23.83	6.65	13.03	15.70	3.65	0.57	17.34
P Phase	14.97	17.13	10.18	16.93	23.03	0.00	0.00	17.13
17	21.15	23.97	7.48	10.28	22.77	2.11	0.37	11.88
P Phase	14.51	17.76	12.55	13.45	27.56	0.00	0.00	14.17
18	22.71	21.71	6.95	11.49	20.73	1.98	0.43	14.01
P Phase	15.52	16.27	11.99	14.37	25.26	0.00	0.00	16.59
19	21.63	22.49	6.94	11.16	20.07	2.33	0.33	15.07
P Phase	14.56	17.09	11.79	14.41	24.34	0.00	0.00	17.82
20	24.46	17.56	1.98	15.02	21.54	1.46	0.21	17.78
P Phase	15.52	12.27	4.02	22.80	27.58	0.00	0.00	17.82
21	21.52	23.76	1.92	14.28	25.05	1.79	0.28	11.42
22F	25.82	18.34	7.57	10.52	24.83	1.39	0.22	11.32
P Phase	18.06	12.59	12.99	12.92	30.34	0.00	0.00	13.11
43F	26.34	15.95	8.29	11.34	20.55	1.91	0.35	15.28
P Phase	17.31	12.92	11.92	14.39	25.22	0.00	0.00	18.24

TABLE B.1(b).—TCP PHASE COMPOSITION WITHIN GRAINS

Alloy	Nickel	Cobalt	Molybdenum	Tungsten	Rhenium	Tantalum	Aluminum	Chromium
1F								
2F								
3F								
4F	54.08	11.31	0.73	5.79	10.13	2.79	9.92	5.25
P Phase	16.89	12.74	3.50	23.69	30.53	0.00	0.00	12.65
5F	40.91	18.87	3.97	8.30	12.40	3.01	6.52	6.02
μ Phase	17.49	18.75	11.37	23.77	20.89	0.07	0.00	7.67
6F								
7F	43.55	17.72	3.35	5.53	9.85	2.30	8.78	8.91
P Phase	15.14	17.29	12.41	13.73	28.38	0.00	0.00	13.05
8F	20.48	23.21	1.77	13.89	19.96	2.98	0.42	17.30
P Phase	12.94	16.79	3.28	23.55	25.94	0.00	0.00	17.50
9F	37.76	13.03	4.91	9.59	15.94	1.75	5.59	11.44
μ Phase	20.18	13.35	10.95	23.35	20.66	0.04	0.00	11.47
P Phase	18.52	12.71	10.45	17.00	24.58	0.00	0.00	16.75
10F	25.25	16.18	7.19	10.20	19.73	1.52	1.02	18.91
P Phase	16.36	13.28	11.69	14.34	25.22	0.00	0.00	19.11
11F	46.53	12.73	3.87	7.46	13.84	2.29	6.57	6.70
	20.62	13.55	11.75	23.73	22.32	0.04	0.00	7.99
12F								
13F								
14F								
15F								
16F	21.78	23.12	6.83	12.73	15.10	2.46	0.88	17.12
P Phase	14.97	17.13	10.18	16.93	23.03	0.00	0.00	17.13
17F	23.14	24.11	7.33	10.09	21.47	2.19	0.47	11.20
P Phase	14.51	17.76	12.55	13.45	27.56	0.00	0.00	14.17
18F	29.58	21.30	5.86	10.50	16.24	2.39	2.57	11.56
P Phase	15.52	16.27	11.99	14.37	25.26	0.00	0.00	16.59
19F	25.00	22.19	6.25	10.73	18.16	2.96	1.11	13.60
P Phase	14.56	17.09	11.79	14.41	24.34	0.00	0.00	17.82
20F	32.50	14.59	1.64	11.81	19.51	1.45	2.78	15.73
P Phase	15.52	12.27	4.02	22.80	27.58	0.00	0.00	17.82
21F	22.51	23.81	1.85	14.19	24.26	1.75	0.41	11.23
22F	36.13	14.25	5.79	8.00	20.84	1.46	4.06	9.48
P Phase	18.06	12.59	12.99	12.92	30.34	0.00	0.00	13.11
43F	28.76	13.90	7.66	10.27	21.04	1.54	1.29	15.54
P Phase	17.31	12.92	11.92	14.39	25.22	0.00	0.00	18.24

TABLE B.2(a).—γ' COMPOSITION AT GRAIN BOUNDARIES

Alloy	Nickel	Cobalt	Molybdenum	Tungsten	Rhenium	Tantalum	Aluminum	Chromium
1	64.89	9.44	0.39	1.52	0.39	3.46	17.86	2.05
	66.44	8.41	0.33	1.33	0.28	4.39	17.56	1.26
2	65.07	9.17	0.37	1.59	0.47	3.60	17.81	1.94
	67.38	7.95	0.29	1.15	0.25	4.98	16.96	1.04
3	65.12	9.17	0.38	1.59	0.38	3.60	17.82	1.94
	66.92	8.17	0.31	1.25	0.27	4.65	17.29	1.14
4	66.80	9.17	0.20	1.86	0.37	3.51	16.06	2.03
	66.64	8.07	0.15	1.61	0.34	4.25	17.65	1.30
5	63.09	12.93	0.63	1.71	0.36	3.83	15.59	1.86
	63.44	11.47	0.45	1.26	0.29	5.16	17.00	0.94
6	63.62	12.52	0.65	1.42	0.37	3.92	15.87	1.65
	64.12	10.95	0.48	1.08	0.28	5.28	16.91	0.90
7	61.76	12.30	0.62	1.22	0.34	3.14	17.73	2.90
	62.69	11.86	0.57	1.28	0.33	4.10	18.08	1.11
8	61.43	13.86	0.15	1.42	0.04	3.73	16.18	3.20
	61.47	12.37	0.11	1.39	0.30	4.63	17.80	1.94
9	66.90	7.71	0.52	1.58	0.26	3.41	17.25	2.38
	67.12	7.28	0.45	1.41	0.23	4.40	17.47	1.64
10	66.45	8.80	0.53	1.19	0.00	3.69	16.51	2.83
	65.99	8.08	0.43	1.12	0.24	4.45	17.74	1.94
11	66.97	8.66	0.63	1.71	0.40	3.65	16.08	1.89
	67.72	7.40	0.47	1.34	0.27	5.00	16.83	0.98
12	66.60	9.53	0.39	1.57	0.02	3.65	16.20	2.05
	66.80	8.19	0.35	1.26	0.27	4.48	17.46	1.19
13	66.91	9.36	0.40	1.57	0.03	3.63	16.08	2.02
	66.86	8.16	0.32	1.26	0.27	4.54	17.40	1.19
14	66.66	9.39	0.37	1.65	0.15	3.60	16.10	2.09
	66.42	8.39	0.34	1.31	0.29	4.32	17.65	1.29
15	68.70	7.99	0.16	1.95	0.02	3.49	15.93	1.76
	68.36	6.90	0.15	1.53	0.31	4.22	17.51	1.02
16	60.39	14.14	0.53	1.29	0.00	3.51	16.79	3.35
	62.49	11.48	0.42	1.35	0.24	4.28	17.94	1.79
17	62.05	13.75	0.67	1.27	0.09	3.52	16.50	2.15
	61.98	12.44	0.55	1.21	0.32	4.20	18.07	1.24
18	63.95	11.75	0.55	1.33	0.00	3.64	16.28	2.51
	63.62	10.68	0.48	1.17	0.26	4.58	17.66	1.54
19	62.66	12.63	0.55	1.21	0.08	4.16	16.09	2.62
	60.24	11.64	0.43	1.08	0.26	4.92	17.50	1.67
20	66.55	8.90	0.19	1.63	0.04	3.06	16.37	3.26
	66.10	7.77	0.17	1.59	0.28	3.65	18.30	2.14
21	62.86	13.44	0.17	1.87	0.01	3.01	16.66	1.98
	62.93	11.58	0.16	1.72	0.35	3.76	18.27	1.22
22	67.11	8.78	0.70	1.47	0.03	3.04	16.94	1.93
	67.27	7.47	0.64	1.34	0.31	3.68	18.11	1.19
23								
24								
25								
26								
27								
28								
29								
30								
31								
32								
33								
34								
35								
36								
37								
38								
39								
40								
41								
42								
43	66.52	7.47	0.52	1.23	0.06	4.07	17.59	2.54
	66.71	7.63	0.43	1.11	0.23	4.86	17.29	1.73
44								

TABLE B.2(b).—γ' COMPOSITION WITHIN GRAINS

Alloy	Nickel	Cobalt	Molybdenum	Tungsten	Rhenium	Tantalum	Aluminum	Chromium
1	64.48	9.32	0.40	1.61	0.53	3.43	17.83	2.39
	66.44	8.41	0.33	1.33	0.28	4.39	17.56	1.26
2	64.24	9.85	0.43	1.65	0.68	3.43	17.25	2.48
	67.38	7.95	0.29	1.15	0.25	4.98	16.96	1.04
3	64.20	9.78	0.42	1.62	0.59	3.47	17.45	2.49
	66.92	8.17	0.31	1.25	0.27	4.65	17.29	1.14
4	66.91	8.99	0.19	1.86	0.41	3.71	15.97	1.95
	66.64	8.07	0.15	1.61	0.34	4.25	17.65	1.30
5	62.43	13.02	0.62	1.74	0.52	3.92	15.78	1.97
	63.44	11.47	0.45	1.26	0.29	5.16	17.00	0.94
6	62.21	13.40	0.74	1.53	0.67	3.74	15.42	2.29
	64.12	10.95	0.48	1.08	0.28	5.28	16.91	0.90
7	60.12	13.62	0.68	1.32	0.61	2.98	17.12	3.56
	62.69	11.86	0.57	1.28	0.33	4.10	18.08	1.11
8	60.42	14.59	0.16	1.61	0.26	3.58	15.49	3.90
	61.47	12.37	0.11	1.39	0.30	4.63	17.80	1.94
9	66.13	8.16	0.57	1.62	0.36	3.34	16.96	2.85
	67.12	7.28	0.45	1.41	0.23	4.40	17.47	1.64
10	64.84	9.52	0.58	1.21	0.17	3.56	16.35	3.78
	65.99	8.08	0.43	1.12	0.24	4.45	17.74	1.94
11	66.52	8.84	0.67	1.80	0.56	3.64	15.88	2.10
	67.72	7.40	0.47	1.34	0.27	5.00	16.83	0.98
12	65.72	10.14	0.41	1.61	0.20	3.52	15.73	2.68
	66.80	8.19	0.35	1.26	0.27	4.48	17.46	1.19
13	64.78	10.65	0.44	1.67	0.37	3.32	15.70	3.07
	66.86	8.16	0.32	1.26	0.27	4.54	17.40	1.19
14	66.00	9.80	0.37	1.64	0.14	3.49	16.11	2.46
	66.42	8.39	0.34	1.31	0.29	4.32	17.65	1.29
15	67.20	9.35	0.21	2.04	0.59	3.05	14.95	2.61
	68.36	6.90	0.15	1.53	0.31	4.22	17.51	1.02
16	58.86	15.10	0.64	1.41	0.15	3.33	16.05	4.46
	62.49	11.48	0.42	1.35	0.24	4.28	17.94	1.79
17	61.98	13.62	0.69	1.30	0.23	3.56	16.45	2.16
	61.98	12.44	0.55	1.21	0.32	4.20	18.07	1.24
18	63.25	12.49	0.59	1.32	0.12	3.50	15.67	3.07
	63.62	10.68	0.48	1.17	0.26	4.58	17.66	1.54
19	62.19	12.81	0.55	1.22	0.12	4.07	16.04	3.00
	60.24	11.64	0.43	1.08	0.26	4.92	17.50	1.67
20	65.68	9.19	0.17	1.73	0.11	3.01	16.36	3.75
	66.10	7.77	0.17	1.59	0.28	3.65	18.30	2.14
21	61.70	14.10	0.21	2.03	0.29	2.96	16.28	2.43
	62.93	11.58	0.16	1.72	0.35	3.76	18.27	1.22
22	66.64	9.21	0.73	1.54	0.24	2.93	16.32	2.41
	67.27	7.47	0.64	1.34	0.31	3.68	18.11	1.19
23								
24								
25								
26								
27								
28								
29	66.67	10.59	0.27	1.70	1.15	3.31	13.15	3.15
	68.11	7.20	0.14	1.20	0.33	4.84	17.15	7.20
30								
31								
32	67.80	9.10	0.21	1.62	0.75	3.78	14.15	2.61
	69.14	6.56	0.14	1.17	0.26	4.56	17.24	0.93
33								
34								
35								
36								
37								
38								
39	62.64	15.13	0.25	1.60	1.16	2.84	13.28	3.09
	65.24	10.15	0.13	1.12	0.29	4.86	17.31	0.90
40								
41								
42								
43	66.33	7.51	0.56	1.26	0.16	4.04	17.40	2.75
	66.71	7.63	0.43	1.11	0.23	4.86	17.29	1.73
44								

TABLE B.3(a).—γ COMPOSITION AT GRAIN BOUNDARIES

Alloy	Nickel	Cobalt	Molybdenum	Tungsten	Rhenium	Tantalum	Aluminum	Chromium
1	59.92	16.51	1.14	2.13	2.50	1.27	9.04	7.50
	58.97	16.39	1.17	2.65	3.17	0.85	9.43	7.38
2	60.65	16.25	1.05	2.21	2.83	1.43	9.04	6.55
	61.19	15.80	1.08	2.57	2.79	1.13	8.97	6.47
3	58.86	17.02	1.09	2.24	3.06	1.26	8.93	7.53
	60.12	16.10	1.13	2.62	2.99	0.97	9.23	6.84
4	59.84	16.94	0.58	2.60	2.97	1.18	7.79	8.11
	59.12	15.76	0.54	3.18	3.70	0.83	9.47	7.41
5	53.85	22.74	1.83	2.47	2.52	1.41	8.25	6.94
	54.05	21.84	1.91	3.06	3.34	0.95	8.78	6.08
6	55.07	22.25	1.92	2.12	2.57	1.41	8.30	6.35
	55.26	21.07	2.02	2.64	3.26	1.01	8.79	5.95
7	51.20	22.59	1.61	1.49	1.87	1.03	10.41	9.80
	52.77	22.13	2.00	2.47	3.61	0.60	9.91	6.51
8	50.90	23.04	0.41	2.04	1.81	1.23	8.89	11.68
	49.51	22.53	0.47	2.67	3.20	0.60	9.46	11.56
9	59.46	14.80	1.68	2.34	2.12	1.11	8.59	9.89
	59.34	13.97	1.73	2.81	2.58	0.91	9.15	9.50
10	57.11	16.29	1.61	1.61	1.63	1.23	8.88	11.65
	56.59	15.27	1.71	2.08	2.71	0.77	9.45	11.43
11	61.59	15.48	1.84	2.54	2.29	1.60	8.36	6.30
	61.32	14.47	1.94	3.22	3.08	1.28	8.59	6.11
12	59.53	17.50	1.13	2.21	2.64	1.30	8.05	7.66
	59.81	16.09	1.24	2.54	3.03	0.90	9.38	7.02
13	59.31	17.56	1.09	2.23	2.69	1.26	8.19	7.68
	59.94	16.05	1.12	2.56	2.99	0.92	9.33	7.09
14	59.86	17.21	1.07	2.27	2.58	1.31	8.22	7.48
	58.89	16.35	1.18	2.55	3.19	0.82	9.53	7.50
15	65.01	13.59	0.42	2.53	2.46	1.76	9.06	5.17
	63.05	13.88	0.48	3.02	3.40	0.95	9.53	5.70
16	51.92	21.72	1.37	1.73	1.00	1.59	10.26	10.41
	51.61	20.96	1.62	2.54	2.64	0.60	9.63	10.40
17	52.73	23.56	1.81	1.65	2.21	1.28	9.14	7.62
	51.42	22.96	1.99	2.33	3.51	0.59	9.89	7.32
18	53.99	20.89	1.75	1.89	2.01	1.18	8.68	9.60
	53.39	19.95	1.90	2.35	2.98	0.72	9.38	9.34
19	52.52	22.01	1.73	1.75	1.87	1.39	8.53	10.21
	51.15	21.48	1.82	2.22	2.92	0.72	9.19	10.50
20	58.25	15.80	0.47	2.18	1.76	1.00	9.02	11.51
	57.33	14.66	0.56	2.58	2.96	0.59	10.07	11.26
21	53.95	23.36	0.49	2.42	2.60	1.00	8.98	7.21
	53.61	21.67	0.53	3.13	3.71	0.54	10.10	6.71
22	61.55	15.56	1.79	1.86	2.24	1.24	9.18	6.59
	60.33	14.57	2.03	2.41	3.49	0.71	9.95	6.52
23								
24								
25								
26								
27								
28								
29								
30								
31								
32								
33								
34								
35								
36								
37								
38								
39								
40								
41								
42								
43	58.81	14.66	1.94	1.89	1.96	1.30	8.63	10.82
	57.96	14.58	1.84	2.27	2.71	0.97	8.98	10.70
44								

TABLE B.3(b).—γ COMPOSITION WITHIN GRAINS

Alloy	Nickel	Cobalt	Molybdenum	Tungsten	Rhenium	Tantalum	Aluminum	Chromium
1	60.52	15.42	1.00	2.21	2.91	1.66	9.85	6.44
	58.97	16.39	1.17	2.65	3.17	0.85	9.43	7.38
2	61.47	15.16	0.96	2.15	2.74	1.80	9.98	5.75
	61.19	15.80	1.08	2.57	2.79	1.13	8.97	6.47
3	61.44	15.46	0.93	2.20	2.67	1.69	9.53	6.08
	60.12	16.10	1.13	2.62	2.99	0.97	9.23	6.84
4	61.88	14.34	0.47	2.52	2.62	2.03	10.27	5.87
	59.12	15.76	0.54	3.18	3.70	0.83	9.47	7.41
5	57.27	19.27	1.50	2.39	2.41	2.28	10.08	4.80
	54.05	21.84	1.91	3.06	3.34	0.95	8.78	6.08
	58.27	18.94	1.53	2.01	2.41	2.32	9.93	4.59
6	55.26	21.07	2.02	2.64	3.26	1.01	8.79	5.95
	52.00	21.35	1.52	1.62	2.09	1.10	10.41	9.91
7	52.77	22.13	2.00	2.47	3.61	0.60	9.91	6.51
	51.29	22.99	0.42	2.04	1.84	1.33	8.82	11.26
8	49.51	22.53	0.47	2.67	3.20	0.60	9.46	11.56
	60.92	13.66	1.49	2.31	1.96	1.51	9.46	8.69
9	59.34	13.97	1.73	2.81	2.58	0.91	9.15	9.50
	57.47	15.72	1.52	1.59	1.47	1.37	9.80	11.06
10	56.59	15.27	1.71	2.08	2.71	0.77	9.45	11.43
	62.54	14.42	1.65	2.55	2.23	1.93	9.22	5.46
11	61.32	14.47	1.94	3.22	3.08	1.28	8.59	6.11
	61.09	16.14	1.00	2.17	2.49	1.73	8.81	6.58
12	59.81	16.09	1.24	2.54	3.03	0.90	9.38	7.02
	61.67	15.66	0.97	2.17	2.28	1.86	9.16	6.24
13	59.94	16.05	1.12	2.56	2.99	0.92	9.33	7.09
	60.62	16.43	1.02	2.28	2.62	1.54	8.59	6.90
14	58.89	16.35	1.18	2.55	3.19	0.82	9.53	7.50
15	65.61	12.93	0.39	2.43	2.35	1.99	9.60	4.69
	63.05	13.88	0.48	3.02	3.40	0.95	9.53	5.70
16	50.66	22.32	1.50	1.81	1.11	1.37	10.04	11.19
	51.61	20.96	1.62	2.54	2.64	0.60	9.63	10.40
17	56.98	19.75	1.44	1.62	1.87	2.12	10.79	5.44
	51.42	22.96	1.99	2.33	3.51	0.59	9.89	7.32
18	55.30	20.23	1.58	1.83	2.08	1.42	8.78	8.78
	53.39	19.95	1.90	2.35	2.98	0.72	9.38	9.34
19	52.79	21.59	1.67	1.79	1.93	1.48	8.79	9.96
	51.15	21.48	1.82	2.22	2.92	0.72	9.19	10.50
20	59.64	14.96	0.42	2.17	1.64	1.28	9.56	10.33
	57.33	14.66	0.56	2.58	2.96	0.59	10.07	11.26
21	55.92	21.10	0.41	2.61	2.83	1.57	9.72	5.83
	53.61	21.67	0.53	3.13	3.71	0.54	10.10	6.71
22	63.61	13.87	1.61	1.85	1.93	1.75	9.97	5.42
	60.33	14.57	2.03	2.41	3.49	0.71	9.95	6.52
29	65.25	12.95	0.40	1.90	2.37	2.45	10.17	4.51
	62.05	14.47	0.51	2.55	3.73	1.11	9.22	6.35
32	65.58	12.64	0.38	1.96	2.55	2.44	9.78	4.67
	64.97	13.45	0.43	2.33	2.84	1.10	9.52	5.37
39	60.98	18.16	0.36	1.70	2.19	2.09	10.19	4.32
	58.02	20.10	0.45	2.34	3.16	0.89	9.52	5.51
43	61.40	12.71	1.65	1.84	1.72	2.03	9.82	8.83
	57.96	14.58	1.84	2.27	2.71	0.97	8.98	10.70

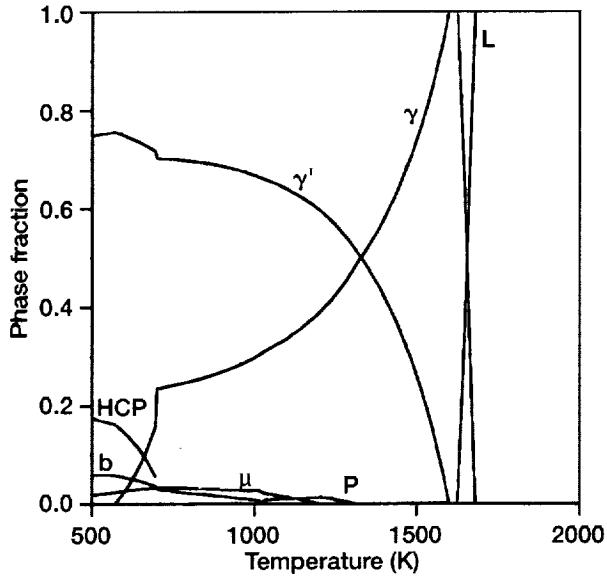

Figure C.1.—Alloy 1.

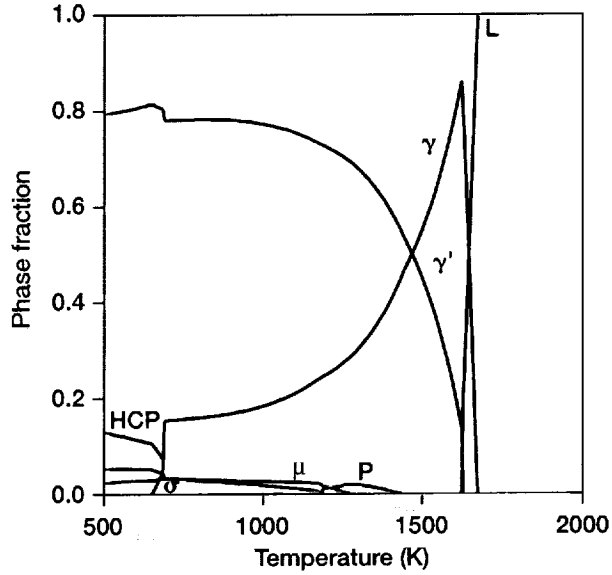

Figure C.2.—Alloy 4.

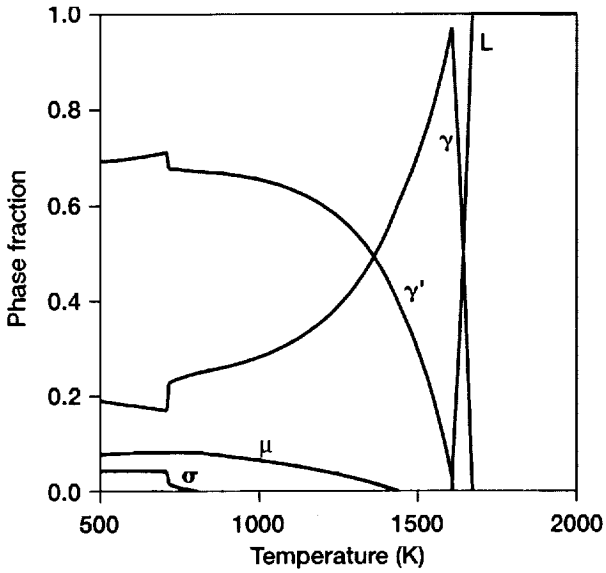

Figure C.3.—Alloy 5.

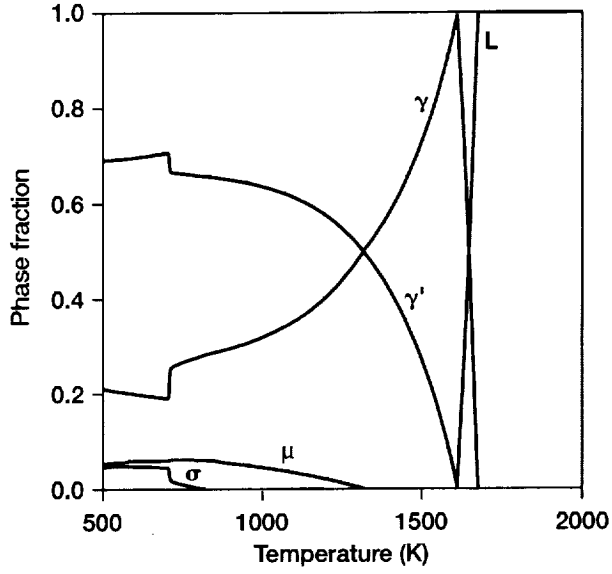

Figure C.4.—Alloy 6.

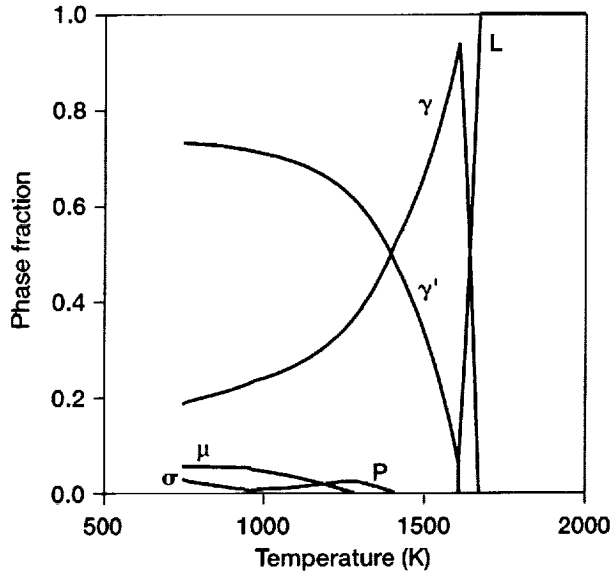

Figure C.5.—Alloy 7.

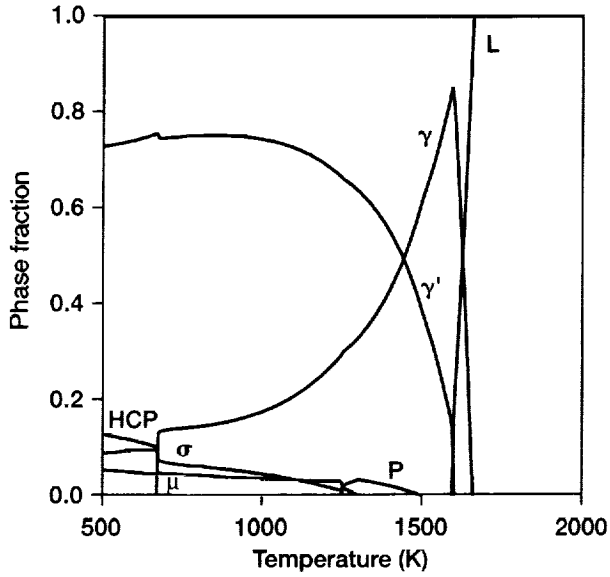

Figure C.6.—Alloy 8.

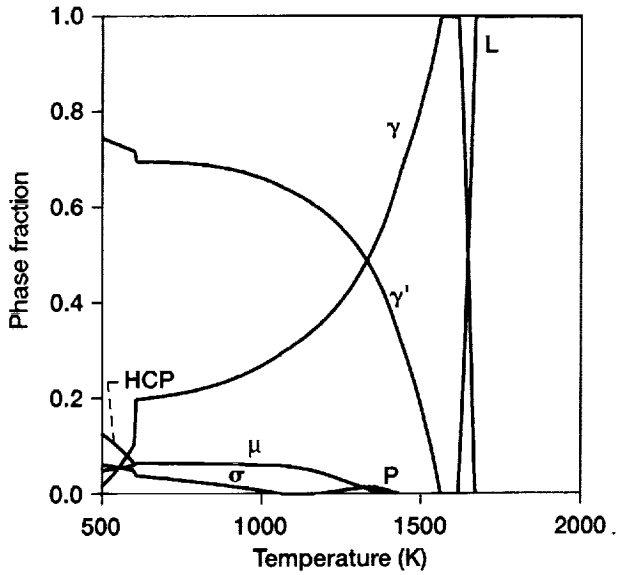

Figure C.7.—Alloy 9.

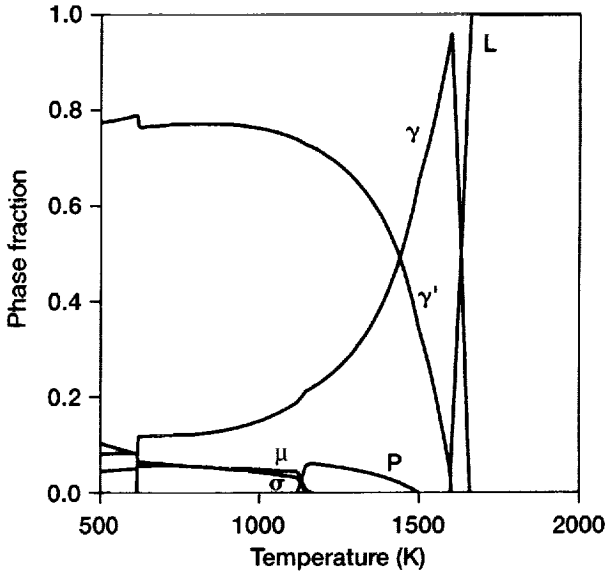

Figure C.8.—Alloy 10.

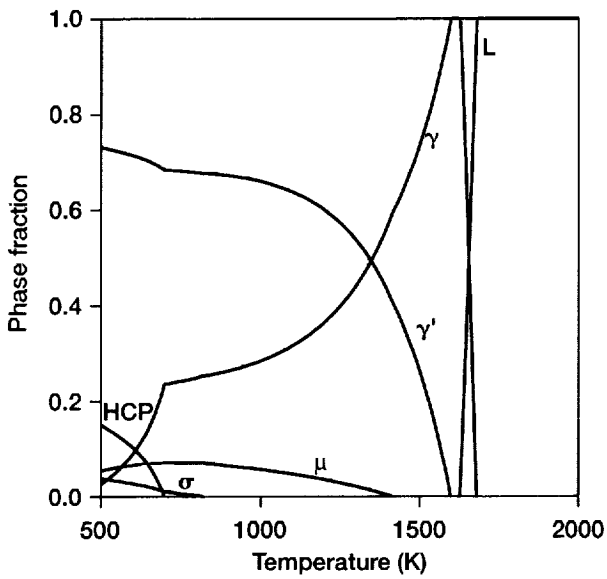

Figure C.9.—Alloy 11.

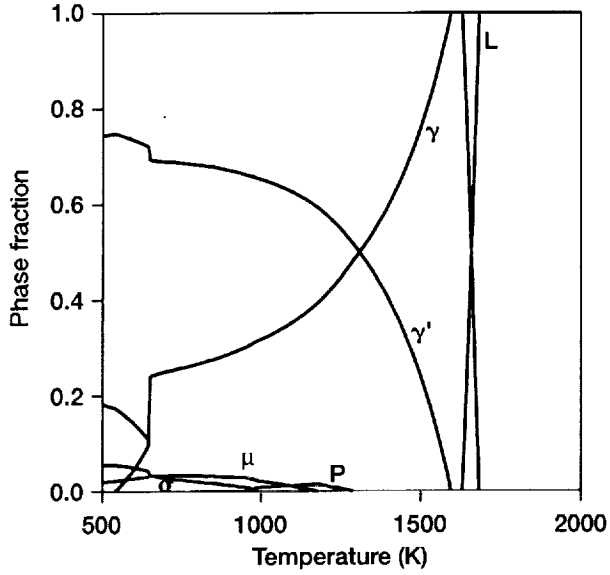

Figure C.10.—Alloy 12.

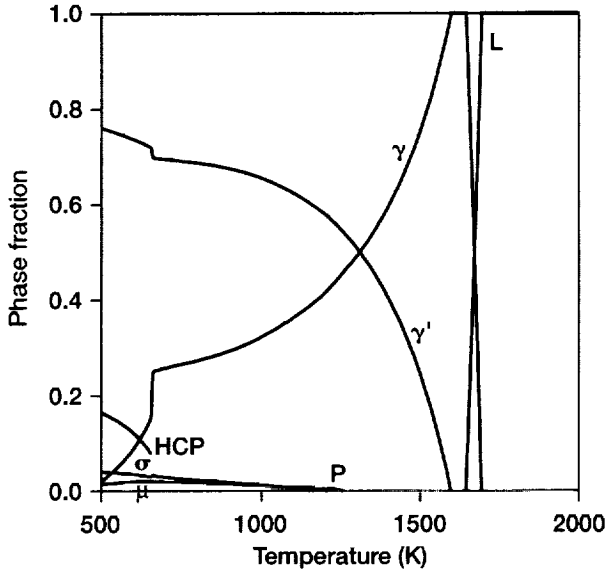

Figure C.11.—Alloy 15.

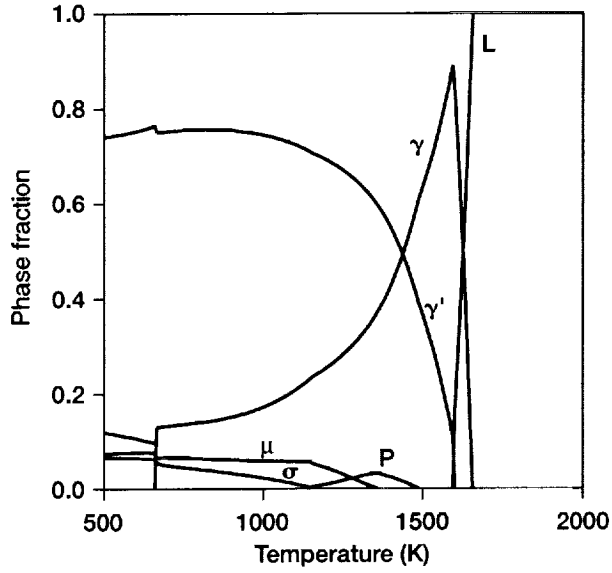

Figure C.12.—Alloy 16.

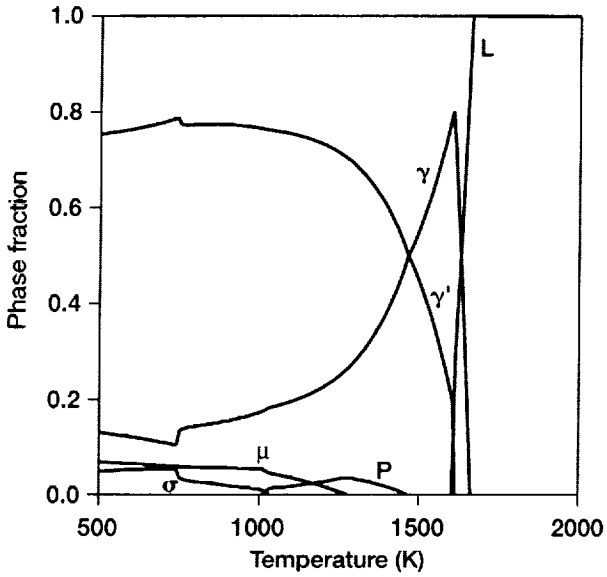

Figure C.13.—Alloy 17.

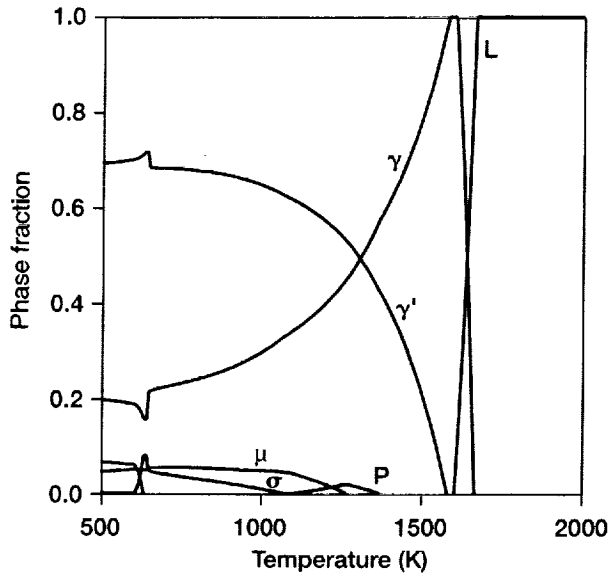

Figure C.14.—Alloy 18.

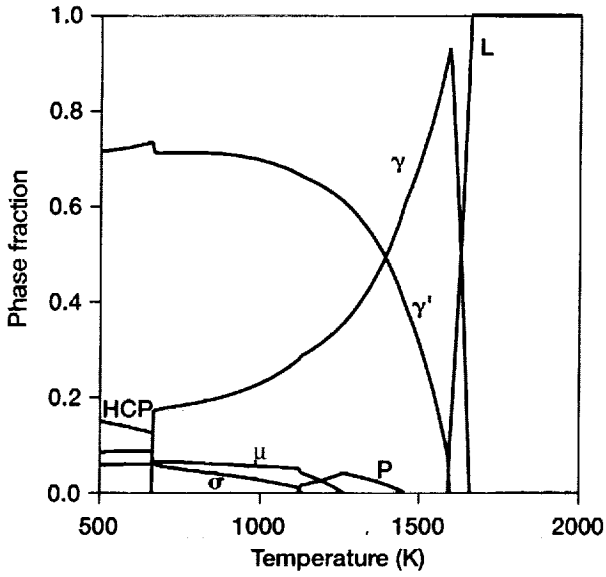

Figure C.15.—Alloy 19.

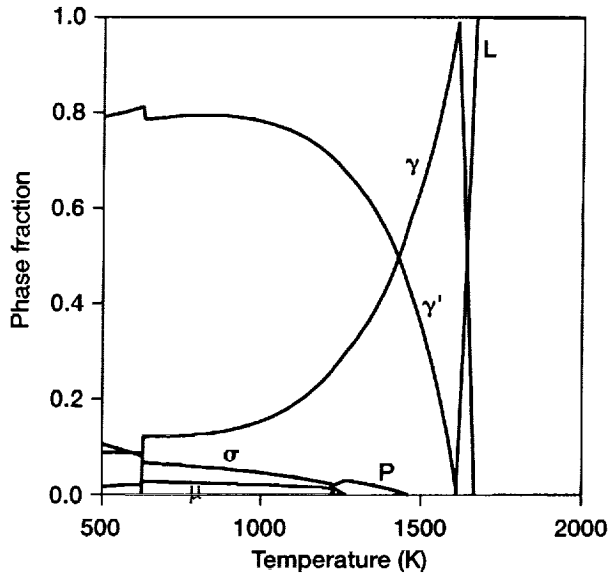

Figure C.16.—Alloy 20.

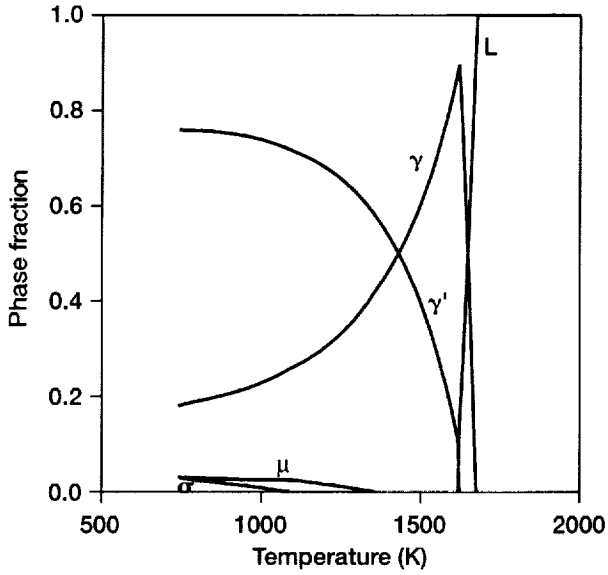

Figure C.17.—Alloy 21.

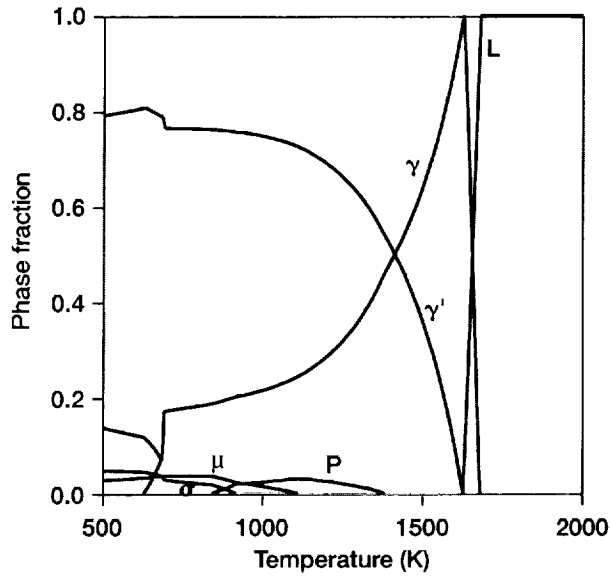

Figure C.18.—Alloy 22.

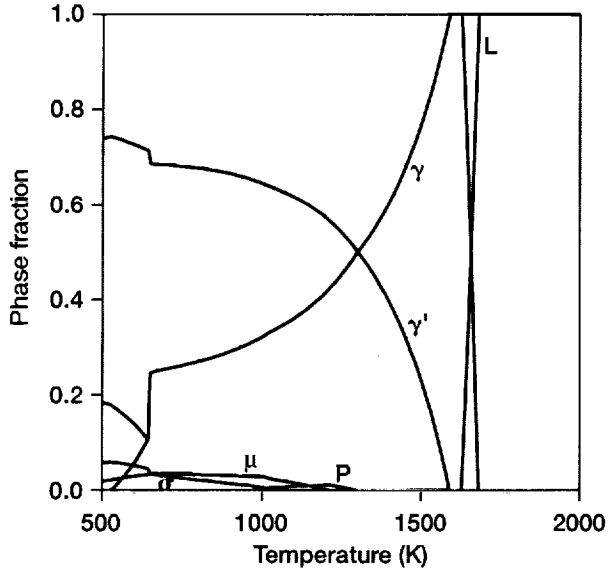

Figure C.19.—Alloy 23.

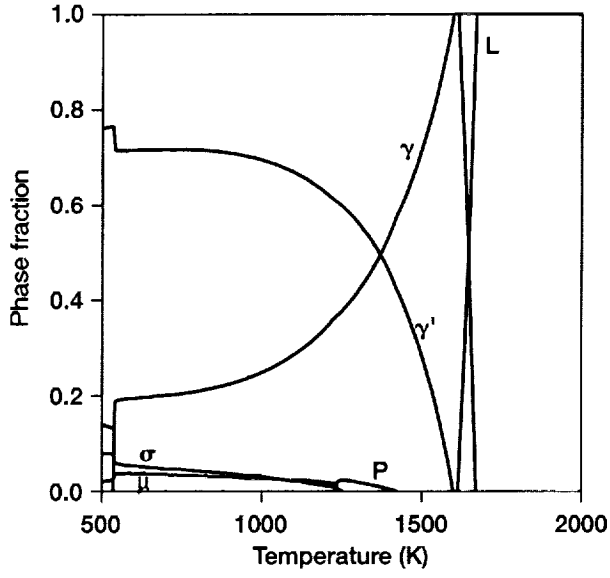

Figure C.20.—Alloy 26.

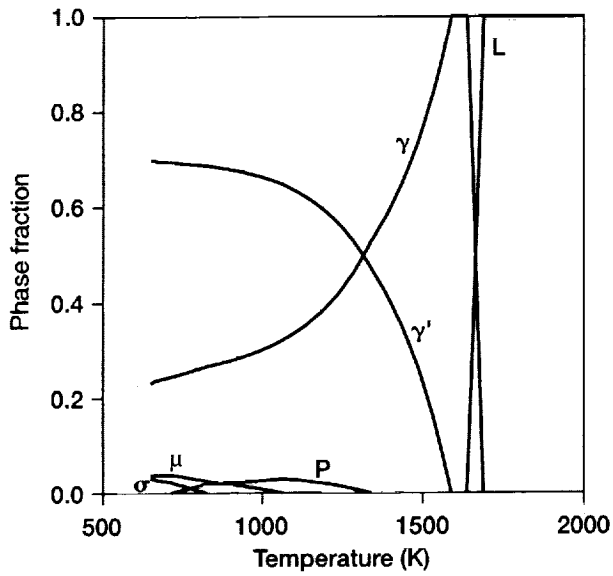

Figure C.21.—Alloy 27.

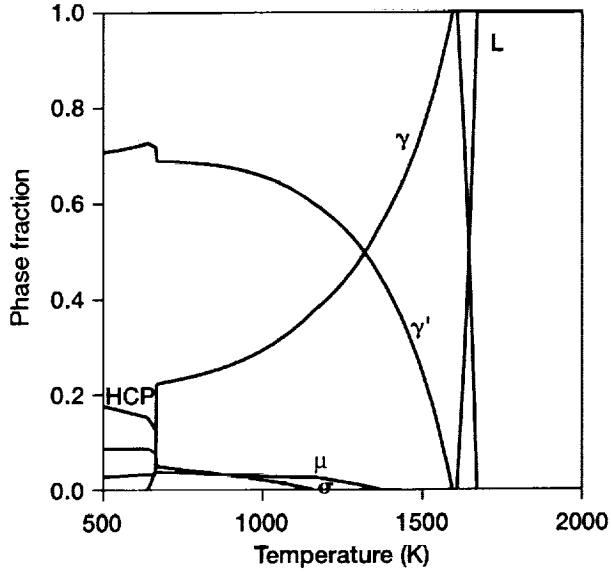

Figure C.22.—Alloy 28.

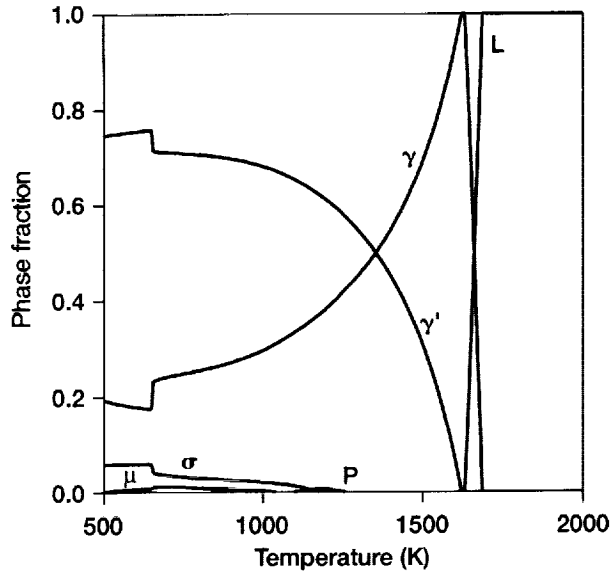

Figure C.23.—Alloy 29.

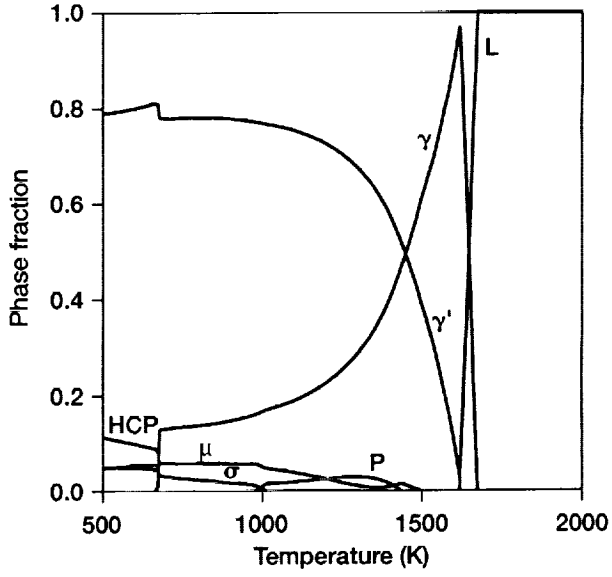

Figure C.24.—Alloy 30.

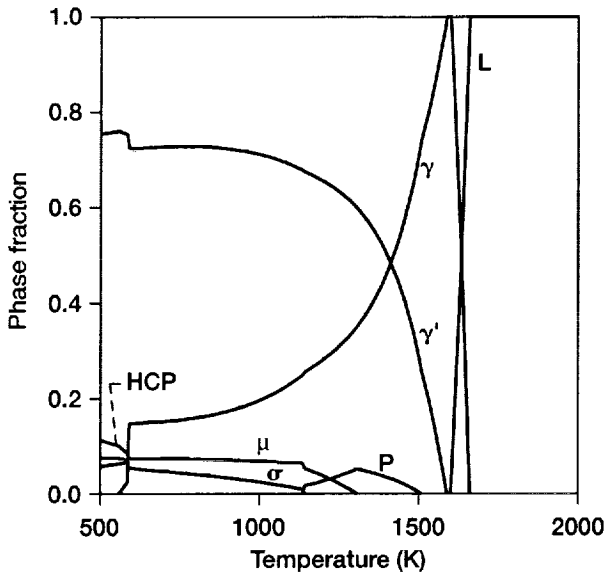

Figure C.25.—Alloy 31.

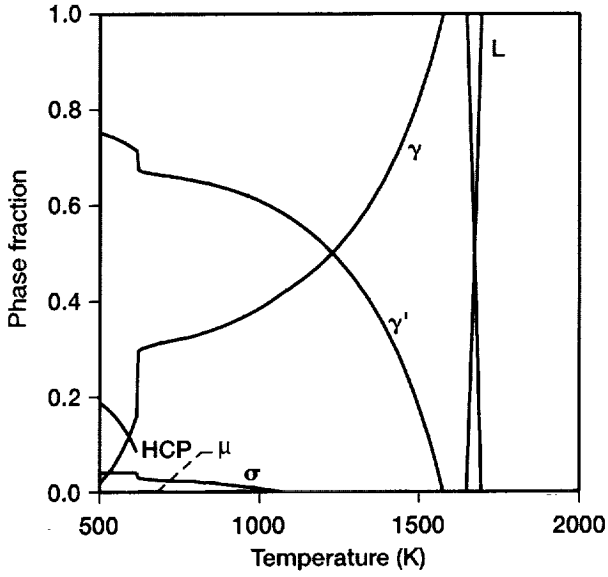

Figure C.26.—Alloy 32.

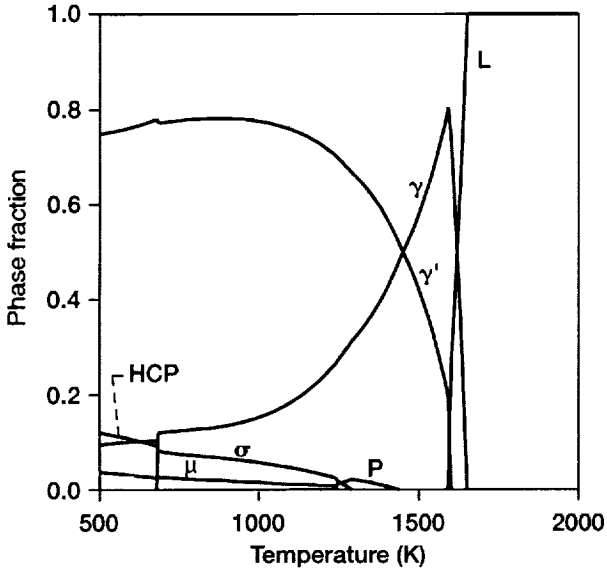

Figure C.27.—Alloy 33.

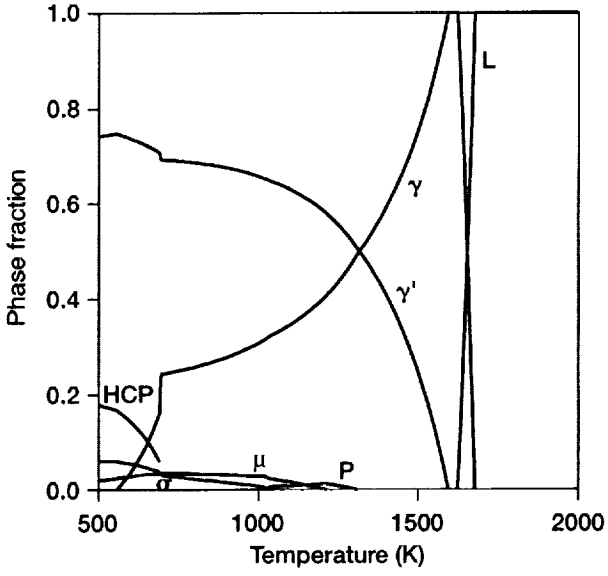

Figure C.28.—Alloy 34.

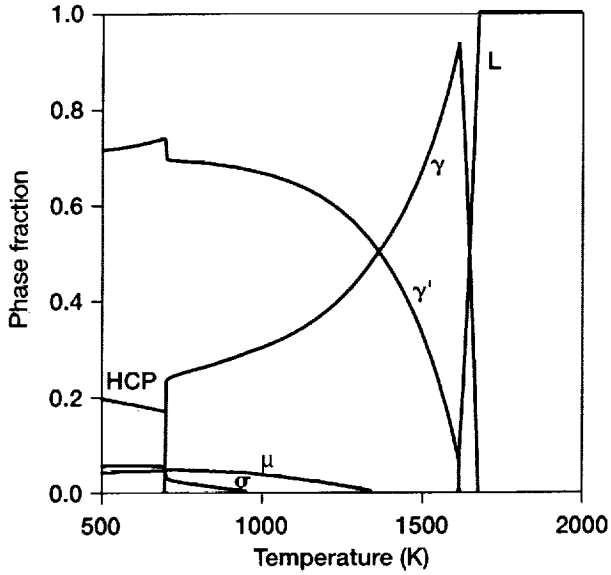

Figure C.29.—Alloy 36.

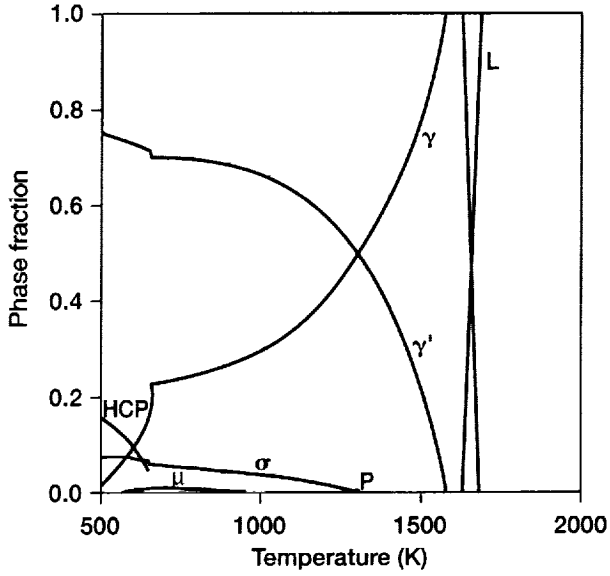

Figure C.30.—Alloy 37.

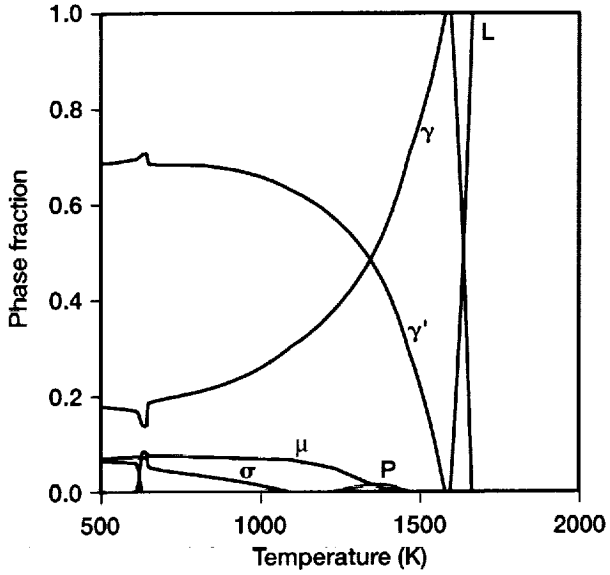

Figure C.31.—Alloy 38.

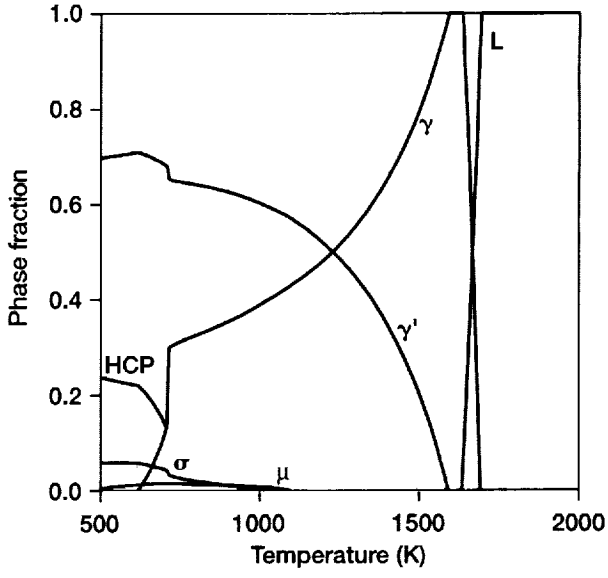

Figure C.32.—Alloy 39.

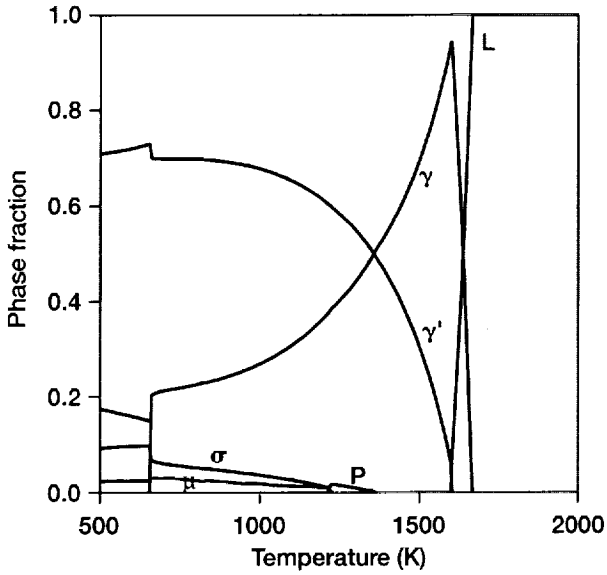

Figure C.33.—Alloy 40.

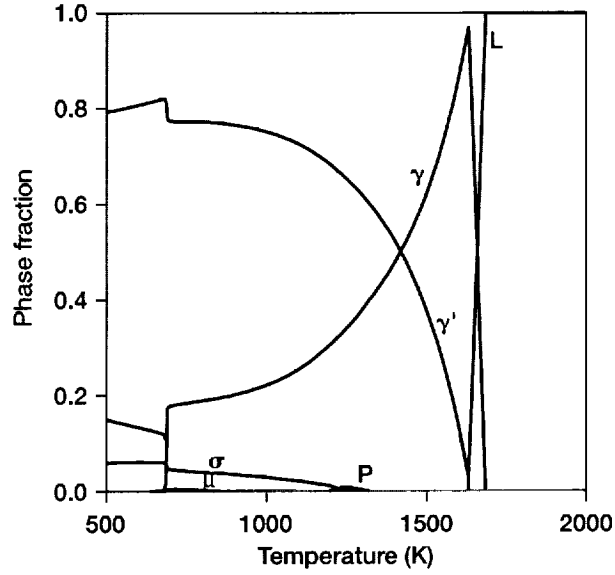

Figure C.34.—Alloy 41.

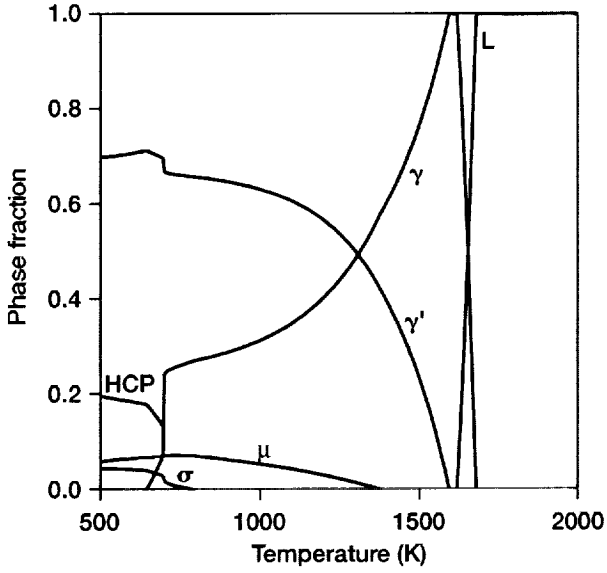

Figure C.35.—Alloy 42.

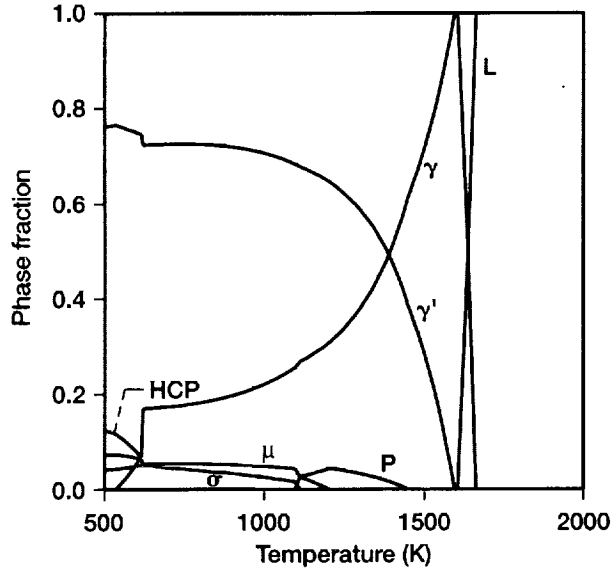

Figure C.36.—Alloy 43.

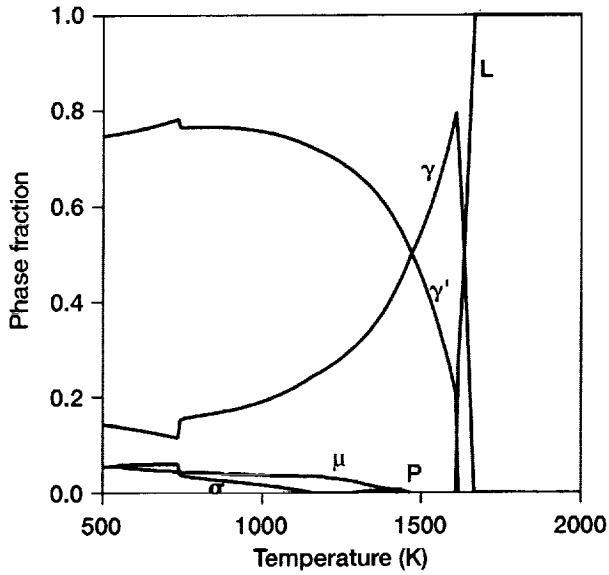

Figure C.37.—Alloy 44.

REFERENCES

1. F. Ritzert, D. Arenas, D. Keller, and V. Vasudevan, "The Effect of Alloying on Topologically Close Packed Phase Instability in Advanced Nickel-Base Superalloy N6," NASA/TM 1998–206622.
2. F. Ritzert, D. Keller, and V. Vasudevan, "Investigation of the Formation of Topologically Close Packed Phase Instabilities in Nickel-Base Superalloy René N6," NASA/TM–1999–209277.
3. C.J. Small and N. Saunders, "The Application of CALPHAD Techniques in the Development of a New Gas-Turbine Disk Alloy," MRS Bulletin, 22–26, April 1999.
4. B. Jansson, M. Schalin, M. Selleby, and B. Sundman, in Computer Software in Chemical and Extractive Metallurgy, edited by C.W. Bale and G.A. Iris, Canadian Institute of Metallurgy, Quebec, 1993, p. 57.
5. W.S. Walston, K.S. O'Hara, T M. Pollock, and W.H. Murphy, "René N6: Third Generation Single Crystal Superalloy," Proceedings of Superalloys Symposium, Seven Springs, PA, September 22–26, 1996.
6. C.M. F. Rae, M.S.A. Karunaratne, C.J. Small, R.W. Broomfield, C.N. Jones, and R.C. Reed, "Topologically Close Packed Phases in an Experimental Rhenium-Containing Single Crystal Superalloy," in Superalloys 2000, edited by T.M. Pollock, R.D. Kissinger, R.R. Bowman, K.A. Green, M. McLean, S. Olson, and J.J. Shirra, The Minerals, Metals, and Materials Society, Warrendale, PA, 2000, pp. 767–776.
7. N. Saunders, M. Fahrmann, and C.J. Small, "The Application of Calphad Calculations to Ni-Based Superalloys," in Superalloys 2000, edited by T.M. Pollock, R.D. Kissinger, R.R. Bowman, K.A. Green, M. McLean, S. Olson, and J.J. Shirra, The Minerals, Metals, and Materials Society, Warrendale, PA, 2000, pp. 803–811.
8. B. Sundman and J. Ågren, "A Regular Solution Model for Phases with Several Components and Sublattices, Suitable for Computer Applications," J. Phys. Chem. Solids, 42, 297–301 (1981).
9. O. Redlich, A.T. Kister, and C.E. Turnquist, "Thermodynamics of Solutions," Chem. Eng. Progress, Symp. Series, 48, 49–64 (1952).
10. M. Hillert, Phase Equilibria, Phase Diagrams and Phase Transformations, Cambridge University Press, Cambridge, 1998, p. 487.
11. F. Ritzert, unpublished work.
12. C.G. Bergeron and S. H. Risbud, Introduction to Phase Equilibria in Ceramics, The American Ceramic Society, Columbus, OH, 1984.

REPORT DOCUMENTATION PAGE

Form Approved
OMB No. 0704-0188

1. AGENCY USE ONLY (Leave blank)	2. REPORT DATE	3. REPORT TYPE AND DATES COVERED
	September 2001	Technical Memorandum

4. TITLE AND SUBTITLE

Computational Thermodynamic Study to Predict Complex Phase Equilibria in the Nickel-Base Superalloy René N6

5. FUNDING NUMBERS

WU–708–31–13–00

6. AUTHOR(S)

Evan H. Copland, Nathan S. Jacobson, and Frank J. Ritzert

7. PERFORMING ORGANIZATION NAME(S) AND ADDRESS(ES)

National Aeronautics and Space Administration
John H. Glenn Research Center at Lewis Field
Cleveland, Ohio 44135–3191

8. PERFORMING ORGANIZATION REPORT NUMBER

E–12775

9. SPONSORING/MONITORING AGENCY NAME(S) AND ADDRESS(ES)

National Aeronautics and Space Administration
Washington, DC 20546–0001

10. SPONSORING/MONITORING AGENCY REPORT NUMBER

NASA TM—2001-210897

11. SUPPLEMENTARY NOTES

Evan H. Copland, National Research Council—NASA Research Associate at Glenn Research Center; Nathan S. Jacobson and Frank J. Ritzert, NASA Glenn Research Center. Responsible person, Nathan S. Jacobson, organization code 5160, 216–433–5498.

12a. DISTRIBUTION/AVAILABILITY STATEMENT

Unclassified - Unlimited
Subject Category: 26 Distribution: Nonstandard

Available electronically at http://gltrs.grc.nasa.gov/GLTRS

This publication is available from the NASA Center for AeroSpace Information, 301–621–0390.

12b. DISTRIBUTION CODE

13. ABSTRACT ***(Maximum 200 words)***

A previous study by Ritzert et al. on the formation and prediction of topologically closed packed (TCP) phases in the nickel-base superalloy René N6 is re-examined with computational thermodynamics. The experimental data on phase distribution in forty-four alloys with a composition within the patent limits of the nickel-base superalloy René N6 provide a good basis for comparison to and validation of a commercial nickel superalloy database used with ThermoCalc. Volume fraction of the phases and partitioning of the elements are determined for the forty-four alloys in this dataset. The baseline heat treatment of 400 h at 1366 K was used. This composition set is particularly interesting since small composition differences lead to dramatic changes in phase composition. In general the calculated values follow the experimental trends. However, the calculations indicated no TCP phase formation when the experimental measurements gave a volume percent of TCP phase less than 2 percent. When TCP phases were predicted, the calculations under-predict the volume percent of TCP phases by a factor of 2 to 8. The calculated compositions of the γ and γ' phases show fair agreement with the measurements. However, the calculated compositions of the P Phase do not agree with those measured. This may be due to inaccuracies in the model parameters for P phase and/or issues with the microprobe analyses of these phases. In addition, phase fraction diagrams and σ and P phase solvus temperatures are calculated for each of the alloys. These calculations indicate that P phase is the primary TCP phase formed for the alloys considered here at 1366 K. Finally, a series of isopleths are calculated for each of the seven alloying elements. These show the effect of each alloying element on creating TCP phases.

14. SUBJECT TERMS	15. NUMBER OF PAGES
Thermodynamics; Alloy phases	45
	16. PRICE CODE

17. SECURITY CLASSIFICATION OF REPORT	18. SECURITY CLASSIFICATION OF THIS PAGE	19. SECURITY CLASSIFICATION OF ABSTRACT	20. LIMITATION OF ABSTRACT
Unclassified	Unclassified	Unclassified	